



ELSEVIER

Contents lists available at ScienceDirect

Spectrochimica Acta Part A: Molecular and Biomolecular Spectroscopy

journal homepage: www.elsevier.com/locate/saa



Spectroscopic (FT-IR, FT-Raman), first order hyperpolarizability, NBO analysis, HOMO and LUMO analysis of 1,7,8,9-tetrachloro-10, 10-dimethoxy-4-[3-(4-phenylpiperazin-1-yl)propyl]-4-azatricyclo [5.2.1.0^{2,6}]dec-8-ene-3,5-dione by density functional methods

R. Renjith ^a, Y. Sheena Mary ^b, C. Yohannan Panicker ^{a,*}, Hema Tresa Varghese ^b, Magdalena Pakońska-Parrys ^c, C. Van Alsenoy ^d, T.K. Manojkumar ^e

The CrossMark logo consists of a blue circular icon containing a red ribbon-like shape that loops back over itself, resembling a bookmark or a ribbon tied in a knot. To the right of the icon, the word "CrossMark" is written in a black, sans-serif font.

^a Department of Physics, TKM College of Arts and Science, Kollam, Kerala, India

^b Department of Physics, Fatima Mata National College, Kollam, Kerala, India

^cDepartment of Medical Chemistry, Medical University of Warsaw, Oczki 3, 02-007 Warszawa, Poland

^d Department of Chemistry, University of Antwerp, B2610 Antwerp, Belgium

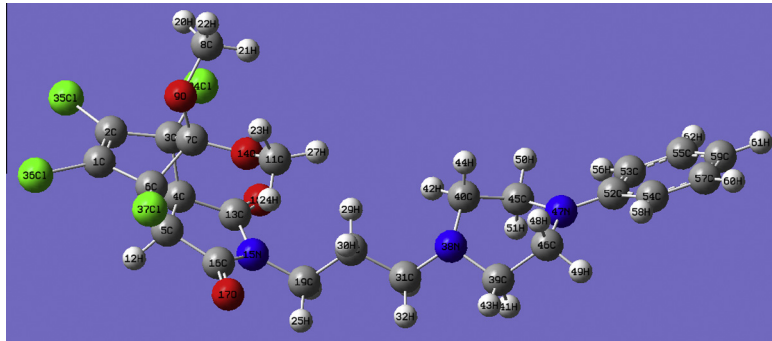
^e Indian Institute of Information Technology and Management-Kerala, Technopark Campus, Trivandrum, Kerala, India

HIGHLIGHTS

GRAPHICAL ABSTRACT

- IR, Raman spectra and NBO analysis were reported.
 - The wavenumbers are calculated theoretically using Gaussian09 software.
 - The wavenumbers are assigned using PED analysis.
 - The geometrical parameters are in agreement with that of similar derivatives.

The optimized molecular structure, vibrational frequencies, corresponding vibrational assignments of 1,7,8,9-tetrachloro-10,10-dimethoxy-4-[3-(4-phenylpiperazin-1-yl)propyl]-4-azatricyclo[5.2.1.0^{2,6}]dec-8-ene-3,5-dione have been investigated experimentally and theoretically using Gaussian09 software package. The HOMO and LUMO analysis is used to determine the charge transfer within the molecule. The stability of the molecule arising from hyper-conjugative interaction and charge delocalization has been analyzed using NBO analysis. Mulliken's net charges have been calculated and compared with the atomic natural charges. First hyperpolarizability is calculated in order to find its role in non-linear optics.



ARTICLE INFO

ABSTRACT

Article history:

Received 20 September 2013

Received in revised form 30 December 2013

Accepted 8 January 2014

Accepted 8 January 2014
Available online 21 January 2014

The optimized molecular structure, vibrational frequencies, corresponding vibrational assignments of 1,7,8,9-tetrachloro-10,10-dimethoxy-4-[3-(4-phenylpiperazin-1-yl)propyl]-4-azatricyclo[5.2.1.0^{2,6}]dec-8-ene-3,5-dione (TDPPAD) have been investigated experimentally and theoretically using Gaussian09 software package. Gauge-including atomic orbital ¹H NMR chemical shifts calculations were carried out and compared with experimental data. The HOMO and LUMO analysis is used to determine the charge transfer within the molecule. The stability of the molecule arising from hyper-conjugative

* Corresponding author. Tel.: +91 9895370968.

E-mail address: cyhyp@rediffmail.com (C.Y. Panicker).

Keywords:
FT-IR
FT-Raman
Azatricyclo
Hyperpolarizability
PED

interaction and charge delocalization has been analyzed using NBO analysis. Molecular Electrostatic Potential was performed by the DFT method and the infrared and Raman intensities have also been reported. Mulliken's net charges have been calculated and compared with the atomic natural charges. First hyperpolarizability is calculated in order to find its role in non-linear optics. The calculated geometrical parameters (SDD) are in agreement with that of similar derivatives.

© 2014 Elsevier B.V. All rights reserved.

Introduction

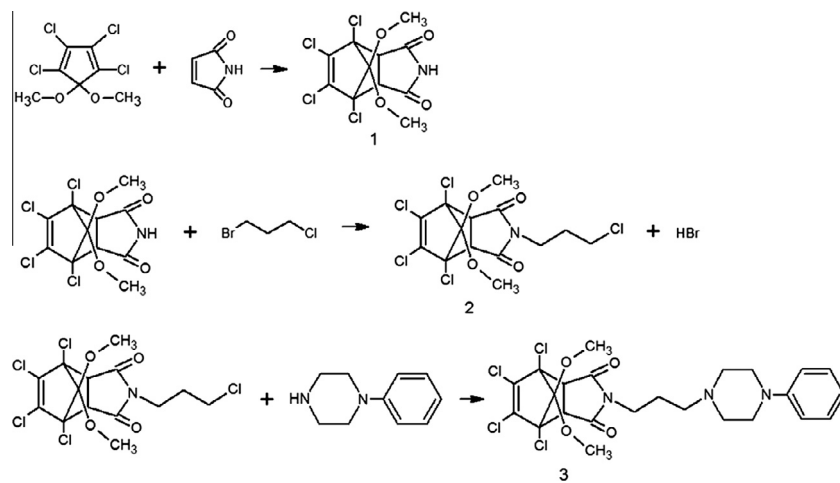
The piperazines or cyclazines are generally considered as ethylenediamine derivatives or cyclic ethylenediamines and are a broad class of chemical compounds with many important pharmacological properties. This di-nitrogen moiety has been an inseparable component of plethora of drugs. Piperazines have the chemical similarity with piperidine, a constituent of piperazine in the black piper plant. Piperazine is introduced into medicine as a solvent for uric acid [1,2]. Recently, piperazine derivatives containing tetrazole nucleus have been reported as an antifungal agent [3]. The piperazine-based research has attracted considerable attention in recent years. Piperazine and substituted piperazine nuclei had constituted an attractive pharmacological scaffold present in various potent marketed drugs. The incorporation of piperazine is an important synthetic strategy in drug discovery due to its easy modifiability, proper alkalinity, water solubility, the capacity for the formation of hydrogen bonds and adjustment of molecular physicochemical properties [4–7]. A broad range of biological active compounds displaying antibacterial [8–11], antifungal [3,12], anticancer [13–15], anti-parasitic [16,17], anti-histamin [18], psychotolytic [19] and anti-depressive activities [20] have been also found to contain this versatile core. In particular, structurally simple 1-(1-naphthylmethyl)-piperazine, as the efflux pump inhibitor, could exert positive effect on tetracyclines and ciprofloxacin against their resistant bacteria [21,22]. Moreover, benzotriazole-based piperazine derivatives and *N,N*-bis(alkyloxymethyl) piperazines had moderate antibacterial and antifungal activities against pathogenic bacterial strains and fungal strains [23,24]. These results once again highlighted that piperazine core was an important backbone and prompted us to design some active molecules with piperazine nucleus. Azatricyclo-dec-8-ene-3,5-dione derivatives have anti bacterial and anti fungal activities with other important biological activities [25]. Panicker et al. [26] reported the quantum chemical DFT study of 4-azatricyclo [5.2.2.0^{2,6}] undecane-3,5,8-trione. Varghese et al. [27] reported the spectroscopic study of

4-(3-bromopropyl)-4-azatricyclo[5.2.2.0^{2,6}] undecane-3,5,8-trione. Kossakowski et al. reported 4-Azatricyclo-[5.2.2.0^{2,6}]-undecane-3,5,8-triones as potential pharmacological agents [28]. Recently 3,8-diazabicyclo-[3.2.1]-octane analogues and 4-azatricyclo[5.2.2.0^{2,6}]-undecane-3,5,8-triones derivatives have been investigated as potential agents for the inhibitory effects of anti-proliferation and HIV-1 multiplication in MT-4 cells respectively [29]. In the present work, IR, Raman and ¹H NMR parameters of the title compound are described both experimentally and theoretically.

Experimental details

1,7,8,9-Tetrachloro-10,10-dimethoxy-4-azatricyclo[5.2.1.0^{2,6}]dec-8-ene-3,5-dione (**1**) was synthesized (scheme 1) as previously described [30]. 1,7,8,9-Tetrachloro-4-(3-chloropropyl)-10,10-dimethoxy-4-azatricyclo[5.2.1.0^{2,6}]dec-8-ene-3,5-dione (**2**) was prepared as follows: A mixture of imide **1** (0.5 g, 0.00138 mol), 1-bromo-3-chloropropane (0.6 g, 0.00415 mol) and anhydrous K₂CO₃ (0.5 g, 0.0036 mol) in acetonitrile (50 mL) was refluxed for 8 h. The inorganic precipitate was filtered off, the solvent was evaporated [31]. The title compound, 1,7,8,9-tetrachloro-10,10-dimethoxy-4-[3-(4-phenylpiperazin-1-yl)propyl]-4-azatricyclo[5.2.1.0^{2,6}] dec-8-ene-3,5-dione (**3**) was prepared as follows: A mixture of compound **2** (0.3 g, 0.0007 mol), 1-phenylpiperazine 0.21 g (0.0013 mol), anhydrous K₂CO₃ (0.3 g, 0.0022 mol) and KI (0.2 g, 0.0012 mol) was dissolved in acetonitrile (50 mL) and refluxed for 30 h. The solvent was evaporated, then the residue was purified by column chromatography (eluent: CH₂Cl₂–CH₃OH, 95:5) [31]. Yield 75%, m.p. 245.5–246 °C. Anal. Calculated: 48.06% C, 4.71% H, 7.01% N; Found: 48.03% C, 4.59% H, 6.80% N.

The FT-IR spectrum (Fig. 1) was recorded using KBr pellets on a DR/Jasco FT-IR 6300 spectrometer. The FT-Raman spectrum (Fig. 2) was obtained on a Bruker RFS 100/s, Germany. For excitation of the spectrum the emission of Nd:YAG laser was used, excitation wavelength 1064 nm, maximal power 150 mW, measurement on solid sample. The ¹H NMR spectra were recorded on a Bruker AVANCE



Scheme 1. Pathway of compound synthesis.

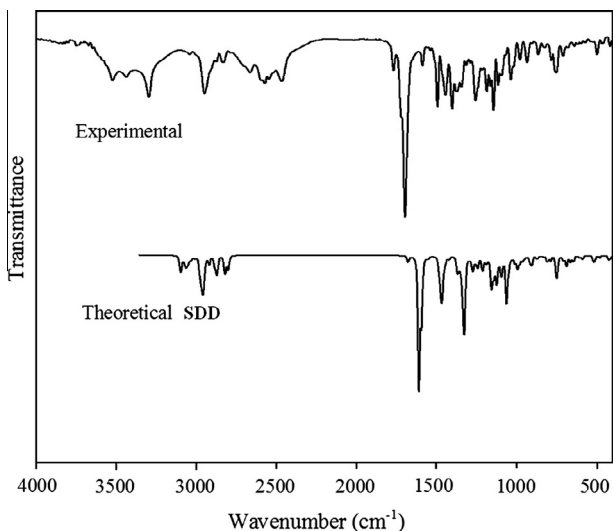


Fig. 1. FT-IR spectrum of TDPPAD.

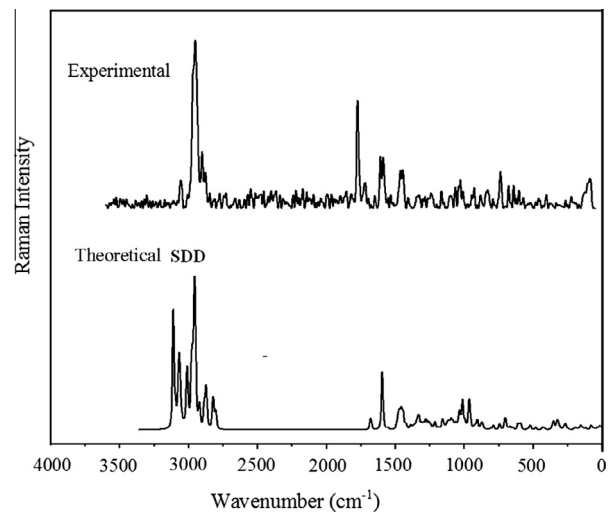


Fig. 2. FT-Raman spectrum of TDPPAD.

DMX 400 spectrometer, operating at 400 MHz. The chemical shift values are expressed in ppm relative to TMS as an internal standard.

Computational details

Calculations of the title compound are carried out with Gaussian09 program [32] using the B3LYP/6-31G* and B3LYP/SDD basis sets to predict the molecular structure and vibrational wavenumbers. Molecular geometry was fully optimized by Berny's optimization algorithm using redundant internal coordinates. Harmonic vibrational wavenumbers were calculated using the analytic second derivatives to confirm the convergence to minima on the potential surface. The DFT hybrid B3LYP functional and SDD methods tend to overestimate the fundamental modes; therefore scaling factor of 0.9613 has to be used for obtaining a considerably better agreement with experimental data [33]. The Stuttgart/Dresden effective core potential basis set (SDD) [34] was chosen particularly because of its advantage of doing faster calculations with relatively better accuracy and structures [35]. Then frequency calculations were employed to confirm the structure as minimum points in energy. Parameters corresponding to optimized geometry (SDD) of the title compound (Fig. 3) are given as Supporting

material in Table S1. The absence of imaginary wavenumbers on the calculated vibrational spectrum confirms that the structure deduced corresponds to minimum energy. The assignments of the calculated wavenumbers are aided by the animation option of GAUSSVIEW program, which gives a visual presentation of the vibrational modes [36]. The potential energy distribution (PED) is calculated with the help of GAR2PED software package [37]. The ¹H NMR data were obtained from the DFT method using basis set 6-31G* and potential energy surface scan studies have been carried out to understand the stability of planar and non-planar structures of the molecule. The HOMO and LUMO are calculated by B3LYP/SDD method.

Results and discussion

IR and Raman spectra

The observed IR and Raman bands and calculated (scaled) wavenumbers and assignments are given in Table 1. In the following discussion, Phenyl ring is designated as R1, piperazine ring is designated as R2, the imido fragment ring is designated as R3 and cyclohexene ring is designated as R4. For the title compound, the assignments of the benzene ring vibrations are made by referring the case of benzene derivatives with mono-substitution as summarized by Roeges [38]. According to Roeges [38], the CH stretching modes for mono-substituted benzene are found in the region 3105–3000 cm⁻¹. For the title compound the bands observed at 3110 cm⁻¹ in the Raman spectrum is assigned as CH stretching mode of the phenyl ring. The calculated (SDD) values are at 3110, 3101, 3094, 3069 and 3062 cm⁻¹. The benzene ring possesses six ring-stretching vibrations, of which the four with the highest wavenumbers occurring respectively near 1600, 1580, 1490 and 1440 cm⁻¹ are good group vibrations. In the absence of ring conjugation, the band near 1580 cm⁻¹ is usually weaker than that at 1600 cm⁻¹. The fifth ring-stretching vibrations ν_{Ph} is active near 1335 ± 35 cm⁻¹ and the intensity is, in general, low or medium high [38,39]. The sixth ring-stretching vibration or ring breathing mode ν_{Ph} appears as a weak band near 1000 cm⁻¹ in mono-substituted benzenes [38]. The bands observed at 1559 and 1496 cm⁻¹ in the IR spectrum and at 1588, 1552 and 1315 cm⁻¹ in the Raman spectrum are assigned as ν_{Ph} ring-stretching modes. As seen from Table 1, the SDD calculations give these modes at 1593, 1553, 1486, 1430, and 1311 cm⁻¹. These vibrations are expected in the region [38] 1620–1300 cm⁻¹. For the title compound, the ring breathing mode is found at 1013 cm⁻¹ theoretically. There are five in-plane bending CH vibrations for mono-substituted benzene. The band observed at 1069 cm⁻¹ in the Raman spectrum is assigned as the in-plane bending vibrations of CH modes. SDD calculations give these modes at 1329, 1184, 1157, 1071 and 1049 cm⁻¹. The out-of-plane CH deformations γ_{CH} of mono-substituted benzene derivative modes are expected in the range [38] 1000–730 cm⁻¹. In general, the γ_{CH} out-of-plane deformations with the highest wavenumbers have a weaker intensity than those absorbing at lower wavenumbers. The stronger γ_{CH} band occurring in the region 775 ± 45 cm⁻¹ (γ_{CH} umbrella mode) tends to shift to lower (higher) wavenumbers with increasing electron donating (attracting) power of the substituent, but seems to be more sensitive to mechanical interaction effects. The lowest wavenumbers for this umbrella mode are found in the spectra of mono-substituted benzene [39–41]. For the title compound the bands at 979 cm⁻¹ in the Raman spectrum and 754 cm⁻¹ in the IR spectrum are assigned as the out-of-plane CH deformations of the phenyl ring. The bands at 980, 959, 872, 814 and 752 cm⁻¹ are the theoretically calculated values for the γ_{CH} deformation modes. The γ_{CH} band at 754 cm⁻¹ in the IR spectrum and the

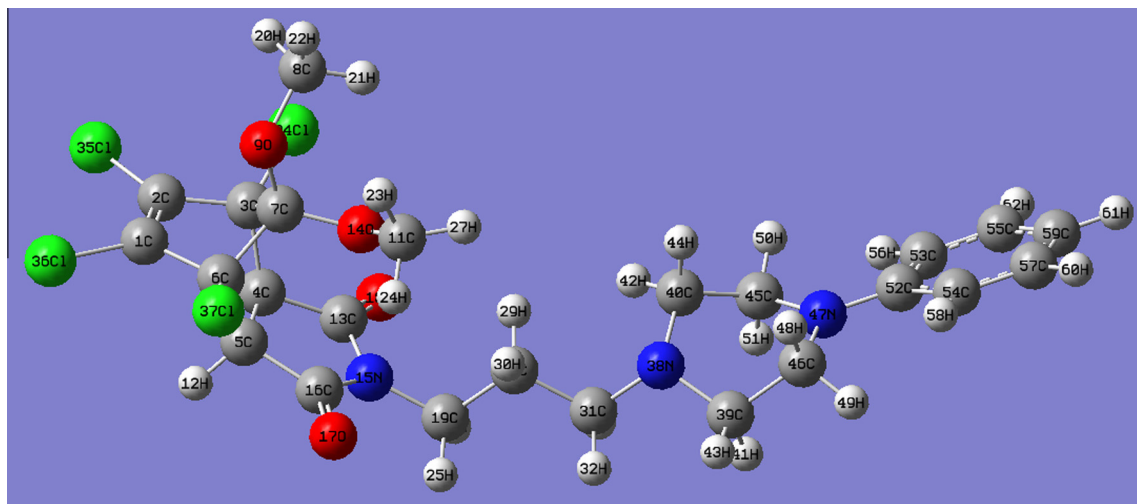


Fig. 3. Optimized geometry (B3LYP/SDD) of TDPPAD.

phenyl ring deformation mode at 500 cm^{-1} in the IR spectrum form a pair of strong bands characteristics of mono-substituted benzene derivatives [38,42].

In aromatic methoxy compounds, $\nu_{as}\text{CH}_3$ are expected in the region [38] 2985 ± 20 and $2955 \pm 20\text{ cm}^{-1}$. For the title compound, computed wavenumbers of modes (SDD) corresponding to the $\nu_{as}\text{CH}_3$ group are 3075, 3065, 3057 and 3047 cm^{-1} . The bands observed at 3042 cm^{-1} in the IR spectrum and at 3081 and 3057 cm^{-1} in the Raman spectrum was assigned as these modes. The symmetrical stretching mode $\nu_s\text{CH}_3$ is expected in the range $2845 \pm 45\text{ cm}^{-1}$ in which all the three CH bonds extend and contract in phase [38]. For the title compound SDD calculations give values 2956 and 2947 cm^{-1} as symmetrical methyl group stretching modes. With methyl esters the overlap of the regions in methyl asymmetrical deformations are active (1465 ± 10 and $1460 \pm 15\text{ cm}^{-1}$) is quite strong, which leads to many coinciding wavenumbers [38]. This is obvious, not only for the asymmetric deformation, but also for the symmetric deformation [38] mostly displayed in the range $1450 \pm 20\text{ cm}^{-1}$. The intensity of these absorptions is only weak to moderate. The SDD calculations give values 1471, 1462, 1457, 1455 cm^{-1} and 1449, 1428 cm^{-1} as $\delta_{as}\text{CH}_3$ and $\delta_s\text{CH}_3$, respectively, for the title compound. The bands observed at 1463 cm^{-1} (Raman) are assigned as the deformation bands of the methyl group. The methyl rocking vibration [38] has been observed at $1190 \pm 45\text{ cm}^{-1}$. The second methyl rock [38] absorb at $1150 \pm 30\text{ cm}^{-1}$. The bands calculated (SDD) at 1158, 1155, 1118 and 1109 cm^{-1} were assigned as rocking modes of the methyl group. These modes are observed at 1118 cm^{-1} in the Raman spectrum.

A methoxy group attached to an aromatic ring give C—O—C stretching modes in the range 1200 – 900 cm^{-1} [40]. The SDD calculation gives 1145, 1065 and 961, 947 cm^{-1} as asymmetric and symmetric C—O—C stretching vibrations. The bands observed at 1145 cm^{-1} in the IR spectrum and at 1148, 1065, 946 cm^{-1} in the Raman spectrum were assigned as C—O—C stretching vibrations. The skeletal C—O deformation can be found in the region [38] $320 \pm 50\text{ cm}^{-1}$. Klimentova et al. [43] reported the asymmetric and symmetric C—O—C stretching vibrations in the range, 1214– 1196 cm^{-1} and 1093– 1097 cm^{-1} . Castaneda et al. [44] reported the methoxy vibrations at 1252, 1190, 1172, 1028 and 1011 cm^{-1} .

The C=O stretching frequency appears strongly in the IR spectrum in the range 1600 – 1700 cm^{-1} because of its large change in dipole moment. The carbonyl group vibrations give rise to characteristic bands in vibration spectra and its characteristic frequency used to study a wide range of compounds. The intensity of these

bands can increase owing to conjugation or formation of hydrogen bonds [45,46]. The carbonyl band of cyclic imides is shifted to higher wavenumber if the ring is strained [46]. The carbonyl groups in the imide fragment give rise to bands [46,48] in the region of 1720 – 1790 cm^{-1} . For the title compound, the C=O stretching bands are observed at 1698 cm^{-1} in the IR spectrum, 1677 , 1609 cm^{-1} in the Raman spectrum and at 1678 , 1611 cm^{-1} theoretically (SDD).

The C—N stretching modes are reported [49] in the range 1100 – 1300 cm^{-1} . Silverstein et al. [50] assigned C—N stretching absorption in the region 1382 – 1266 cm^{-1} for aromatic amines. In the present case, the ν_{CN} stretching modes are observed at 1328 cm^{-1} in the Raman spectrum and at 1338 , 1335 , 1325 , 1140 , 1124 cm^{-1} theoretically corresponding to $\text{C}_{52}\text{—N}_{47}$, $\text{C}_{13}\text{—N}_{15}$, $\text{C}_{16}\text{—N}_{15}$, $\text{C}_{19}\text{—N}_{15}$ and $\text{C}_{31}\text{—N}_{38}$ respectively. Kas'yan et al. [51] reported the CN stretching in the region 1350 – 1100 cm^{-1} and Nakanishi [48] reported the range as 1300 – 1200 cm^{-1} .

For bridging methylene groups [47] the CH_2 (at C_{19} , C_{28} , C_{31}) vibrations are observed in the region of 2800 – 3000 , 1200 – 1400 , 875 – 1150 and 600 – 850 cm^{-1} . The vibrations of these CH_2 groups (the asymmetric stretch $\nu_{as}\text{CH}_2$, symmetric stretch $\nu_s\text{CH}_2$, the scissoring vibration and wagging vibration) appear in the regions of 2940 – 3005 , 2870 – 2940 , 1420 – 1480 and 1320 – 1380 cm^{-1} , respectively [38,40,52]. These bands are observed at 2949 cm^{-1} in the IR spectrum, 3028 , 3008 , 2966 , 2951 , 2811 cm^{-1} in the Raman spectrum and in the ranges of 3031 – 2965 , 2954 – 2801 , 1473 – 1419 , 1390 – 1298 cm^{-1} theoretically (SDD) for the title compound respectively. According to literature [50] scissoring mode of the CH_2 group give rise to characteristic band near 1465 cm^{-1} in IR and Raman spectra. These modes are unambiguously correlated with the strong bands in the region of 1402 – 1482 cm^{-1} observed experimentally. The twisting and rocking vibrations of the CH_2 group appear in the region [38] of 1200 – 1280 and 740 – 900 cm^{-1} , respectively. These modes are also assigned (Table 1). For the title compound the twisting vibrations are observed at 1290 cm^{-1} in the IR spectrum, 1285 , 1242 cm^{-1} in the Raman spectrum and at 1283 , 1244 , 1236 cm^{-1} theoretically. The rocking deformations are observed at 868 , 825 cm^{-1} in the IR spectrum, 830 cm^{-1} in the Raman spectrum and at 867 , 833 , 809 cm^{-1} theoretically and these modes are not pure, but contain significant contributions from other modes also. In the bridging methylene group, for $\text{C}_{28}\text{—C}_{31}$ and $\text{C}_{19}\text{—C}_{28}$, C—C stretching modes are found at 1037 and 1020 cm^{-1} respectively.

The hydrocarbon CH stretching vibrations occur [40] above 2900 cm^{-1} and CH deformations absorb weakly in the region of

Table 1

IR, Raman bands and calculated (scaled) wavenumbers of TDPPAD and assignments.

B3LYP/6-31G*			B3LYP/SDD IR			Raman		Assignments ^a	
v	IR _I	R _A	v	IR _I	R _A	v	v		
3107	0.32	270.37	3110	2.59	304.37	—	3110	vCH (R ₁) (99)	
3103	29.49	4.39	3101	38.05	1.44	—	—	vCH (R ₁) (94)	
3093	50.50	108.04	3094	50.91	50.02	—	—	vCH (R ₁) (95)	
3074	9.92	62.93	3075	14.86	57.78	—	3081	v _{as} CH ₃ (96)	
3069	18.68	135.91	3069	15.67	111.77	—	—	vCH (R ₁) (100)	
3065	12.28	79.50	3065	18.03	66.09	—	—	v _{as} CH ₃ (99)	
3063	9.00	48.11	3062	9.02	34.13	—	—	vCH (R ₁) (93)	
3059	9.24	29.49	3057	16.85	27.75	—	3057	v _{as} CH ₃ (93)	
3046	17.21	23.20	3047	27.15	20.16	3042	—	v _{as} CH ₃ (98)	
3023	11.44	11.84	3031	18.87	7.93	—	3028	v _{as} CH ₂ (98)	
3005	1.39	127.20	3013	3.05	132.73	—	—	vC ₄ —H ₁₀ (53), vC ₅ —H ₁₂ (47)	
2998	9.84	40.97	3007	9.86	36.82	—	3008	v _{as} CH ₂ (97)	
2996	0.80	35.14	3002	0.69	28.53	—	—	vC ₄ —H ₁₀ (47), vC ₅ —H ₁₂ (53)	
2969	22.52	64.66	2980	41.51	96.78	—	—	v _{as} CH ₂ (R ₂) (95)	
2966	21.02	96.71	2972	22.51	88.15	—	—	v _{as} CH ₂ (R ₂) (95)	
2963	28.11	31.31	2968	67.52	47.17	—	—	v _{as} CH ₂ (R ₂) (90)	
2960	40.91	145.28	2965	38.81	35.58	—	2966	v _{as} CH ₂ (96)	
2957	22.18	78.31	2957	59.90	60.52	—	—	v _{as} CH ₂ (R ₂) (75), vCH ₂ (11)	
2957	51.49	28.12	2956	38.25	205.75	—	—	v _s CH ₃ (88)	
2951	11.52	51.26	2954	8.76	32.05	—	—	v _s CH ₂ (79), v _s CH ₂ (R ₂) (6)	
2948	44.36	131.77	2950	3.73	55.75	2949	2951	v _s CH ₂ (89), v _s CH ₂ (R ₂) (6)	
2942	4.31	37.86	2947	34.92	93.41	—	—	v _s CH ₃ (100)	
2912	41.37	56.86	2921	40.19	65.75	—	2902	v _s CH ₂ (R ₂) (95)	
2878	50.92	74.66	2884	55.99	80.14	—	2878	v _s CH ₂ (R ₂) (96)	
2864	69.20	110.47	2870	84.52	115.44	2873	—	v _s CH ₂ (R ₂) (91)	
2812	83.25	102.26	2822	98.37	102.38	2831	2822	v _s CH ₂ (R ₂) (91)	
2790	64.79	55.38	2801	64.22	50.69	—	2811	v _s CH ₂ (94)	
1709	29.05	19.60	1678	32.91	26.97	1698	1677	vC=O (77), δR ₃ (11)	
1643	433.08	0.32	1611	501.17	0.63	—	1609	vC=O (77)	
1611	47.09	23.39	1594	15.30	22.27	1589	—	vC=C (R ₄) (57), vC—C (R ₁) (10)	
1603	176.87	92.06	1593	256.96	94.03	—	1588	vC—C (R ₁) (62), vC=C (R ₄) (22)	
1566	10.82	3.69	1553	12.65	3.04	1559	1552	vC—C (R ₁) (67)	
1511	20.57	15.64	1486	30.21	10.75	1496	—	vC—C (R ₁) (77)	
1506	30.01	13.14	1481	34.34	8.84	—	—	δ _{as} CH ₂ (R ₂) (60), δ _{as} CH ₂ (12)	
1500	14.61	4.87	1476	6.18	3.20	—	—	δ _{as} CH ₂ (R ₂) (80), δ _{as} CH ₂ (11)	
1492	42.48	10.96	1473	23.58	7.99	—	—	δ _{as} CH ₂ (64)	
1490	41.31	7.92	1471	25.70	8.21	—	—	δ _{as} CH ₃ (84)	
1489	48.13	48.13	1468	151.44	8.86	—	—	δ _{as} CH ₂ (R ₂) (62)	
1488	28.68	15.35	1466	16.62	4.68	—	—	δ _{as} CH ₂ (R ₂) (74), δ _{as} CH ₂ (16)	
1483	23.56	7.97	1462	33.64	4.89	—	1463	δ _{as} CH ₃ (91)	
1477	1.97	18.83	1457	4.74	9.41	—	—	δ _{as} CH ₃ (41), δCH ₂ (29), δ _{as} CH ₂ (R ₂) (13)	
1474	6.21	20.52	1455	8.18	17.78	—	—	δ _{as} CH ₃ (39), δCH ₂ (37), δ _{as} CH ₂ (R ₂) (9)	
1469	9.77	7.43	1449	13.84	3.44	—	—	δ _s CH ₃ (83)	
1461	16.23	34.97	1444	14.07	28.93	1445	1445	δ _{as} CH ₂ (90)	
1457	0.05	2.56	1430	0.08	2.79	—	—	δCH (R ₁) (20), vC—C (R ₁) (44)	
1441	4.57	4.84	1428	5.96	3.14	—	—	δ _s CH ₃ (91)	
1429	4.87	9.44	1419	8.91	5.75	1404	1409	δ _{as} CH ₂ (93)	
1403	1.85	6.74	1390	1.56	8.28	1379	—	δ _s CH ₂ (44), δ _s CH ₂ (R ₂) (33)	
1386	15.98	1.68	1370	45.87	4.98	1371	—	δ _s CH ₂ (R ₂) (52), δ _s CH ₂ (11)	
1383	111.67	3.78	1368	41.29	2.18	—	—	δ _s CH ₂ (48), δ _s CH ₂ (R ₂) (15)	
1372	2.32	6.11	1358	0.75	2.61	—	—	δ _s CH ₂ (R ₂) (57)	
1365	13.42	7.52	1353	44.67	3.82	—	—	δ _s CH ₂ (R ₂) (35), δ _s CH ₂ (24)	
1356	8.07	8.42	1345	10.70	6.34	1346	1345	δ _s CH ₂ (R ₂) (53), δ _s CH ₂ (12)	
1354	51.23	15.74	1338	54.14	14.36	—	—	vC ₅₂ —N ₄₇ (52), δ _s CH ₂ (R ₂) (12), δCH (R ₁) (10)	
1351	78.87	4.35	1335	122.85	4.42	—	—	δCH ₂ (10), δC ₁₃ —N ₁₅ (R ₃) (48)	
1349	81.94	10.61	1329	5.04	5.78	—	—	δCH (R ₁) (62), δCH (R ₂) (8)	
1334	253.65	14.26	1325	248.21	12.51	—	1328	vC ₁₆ —N ₁₅ (R ₃) (46), δ _s CH ₂ (17)	
1314	1.88	6.25	1311	2.12	7.61	—	1315	vC—C (R ₁) (63)	
1310	5.39	15.80	1298	6.80	10.29	—	1301	δ _s CH ₂ (56), δ _s CH ₂ (R ₂) (11)	
1299	6.02	12.19	1283	13.65	10.72	1290	1285	δCH ₂ (48), δCH ₂ (R ₂) (23)	
1295	15.45	6.32	1281	8.91	3.76	—	—	δC ₄ —H ₁₀ (66), δC ₅ —H ₁₂ (8)	
1288	43.54	8.03	1274	30.51	4.81	—	—	δCH ₂ (R ₂) (52), δCH ₂ (32)	
1282	23.95	9.69	1270	24.72	6.15	—	—	δC ₅ —H ₁₂ (66), δC ₄ —H ₁₀ (8)	
1267	14.78	10.92	1255	23.46	13.98	1259	1264	δCH ₂ (R ₂) (37), δCH ₂ (27)	
1257	55.40	8.10	1244	48.00	4.903	—	1242	δCH ₂ (69)	
1247	0.83	4.33	1236	1.09	2.04	—	—	δCH ₂ (72)	
1232	33.17	5.81	1220	11.96	2.10	1217	1226	δCH ₂ (R ₂) (43), vC—N (R ₂) (19)	
1227	56.30	10.31	1213	58.02	12.82	—	—	δCH ₂ (R ₂) (52)	
1206	14.21	3.23	1195	14.35	1.37	—	1201	vC—C (R ₃) (48)	
1201	4.18	3.67	1187	19.68	1.44	1188	1186	vC—C (R ₃) (48), δC ₅ —H ₁₂ (14), δC ₄ —H ₁₀ (23)	
1191	20.46	1.58	1184	5.87	2.69	—	—	δCH (R ₁) (77), vC—C (R ₁) (15)	
1176	4.51	7.61	1161	62.77	4.74	1165	1166	vC ₄₀ —N ₃₈ (R ₂) (31), δCH ₂ (10)	
1167	69.55	5.29	1158	58.15	5.18	—	—	δCH ₃ (42), vC ₇ —O ₉ (17)	

Table 1 (continued)

B3LYP/6-31G*			B3LYP/SDD IR			Raman		Assignments ^a	
v	IR _I	R _A	v	IR _I	R _A	v	v		
1163	13.28	5.52	1157	7.36	4.28	–	–	δCH (R ₁) (61)	
1160	64.05	1.06	1155	8.52	4.17	–	–	δCH ₃ (68)	
1152	101.24	4.10	1145	83.37	4.09	1145	1148	v _{as} C—O—C (42), δCH ₃ (29), vC ₆ —C ₇ (10)	
1143	6.28	2.52	1140	19.33	2.17	–	–	vC ₁₉ —N ₁₅ (34), vC—C (R ₃) (14)	
1135	49.46	6.63	1126	44.57	2.18	–	–	vC—C (R ₄) (41), δR ₄ (12)	
1129	62.31	1.33	1124	70.33	5.79	–	–	vC ₃₁ —N ₃₈ (25), δCH ₂ (R ₂) (12)	
1126	17.39	4.56	1118	7.35	5.41	–	1118	δCH ₃ (75)	
1116	15.24	9.75	1109	8.40	9.64	–	–	δCH ₃ (60), vC—C (R ₄) (16)	
1106	46.15	4.51	1099	44.45	5.56	1096	1096	vC ₃₉ —N ₃₈ (48), δCH ₂ (23), δCH ₂ (R ₂) (6)	
1098	64.25	11.42	1093	64.08	15.77	–	–	vC—C (R ₄) (40), δCH ₃ (10)	
1089	7.81	6.15	1081	2.53	8.46	–	–	vC—C (R ₃) (52), δCH ₂ (R ₂) (16)	
1087	0.50	1.49	1071	3.22	1.28	–	1069	δCH (R ₁) (32), vC—C (R ₁) (17)	
1078	147.09	7.14	1065	140.01	5.60	–	1065	v _{as} C—O (45), δC—O (13)	
1069	0.75	3.87	1062	48.91	3.78	–	–	vC—C (R ₃) (31), vC ₁₉ —N ₁₅ (21), vC—C (R ₄) (20)	
1061	35.74	2.36	1054	23.24	2.76	–	–	vC—C (R ₄) (41), δCH ₂ (R ₂) (26)	
1057	35.84	3.89	1049	26.73	2.38	–	–	δCH (R ₁) (37), δCH ₂ (R ₄) (7)	
1039	5.16	18.78	1037	5.49	25.07	1038	1042	vC ₂₈ —C ₃₁ (43), δCH ₂ (R ₂) (15), δCH ₂ (20),	
1035	8.72	10.03	1031	9.12	9.76	–	1029	vC—C (R ₂) (41), vC ₂₈ —C ₃₁ (6), δCH ₂ (R ₂) (15)	
1029	10.65	21.70	1020	1.61	7.31	1019	–	vC ₁₉ —C ₂₈ (51), vC ₂₈ —C ₃₁ (6)	
1016	1.84	8.84	1013	6.97	26.86	–	–	vC—C (R ₁) (50)	
1015	15.12	4.62	1011	19.40	15.60	–	1011	vC—C (R ₃) (40), δC—O (12)	
993	76.95	7.07	995	52.75	11.30	–	999	γCH (42), vC—C (R ₄) (13)	
986	11.21	37.08	982	27.57	1.20	981	–	vC—N (R ₂) (33), δCH ₂ (R ₂) (16)	
982	2.50	11.22	980	1.10	1.47	–	979	γCH (R ₁) (75), τC—C—C—C (R ₁) (14)	
972	0.43	1.01	966	9.73	31.24	–	964	γCH (44), vC—C (R ₁) (12)	
969	12.33	2.85	962	5.59	2.80	–	–	vC—C (R ₄) (65)	
960	11.78	5.55	961	9.92	7.79	–	–	v _s C—O—C (33), vC—C (15), τR ₄ (12)	
948	8.02	4.92	959	1.13	13.16	–	–	γCH (R ₁) (75), δC—C—C (R ₁) (10)	
943	0.20	1.69	947	9.58	3.85	–	946	v _s C—O—C (39), vC—C (R ₃) (10)	
931	5.11	5.12	926	4.12	3.83	936	928	vC—C (R ₂) (33)	
915	41.01	5.38	915	40.79	7.74	–	–	δCH ₂ (R ₂) (55), vC—O (18)	
912	34.61	12.56	903	25.79	12.27	905	906	vC ₄₅ —N ₄₇ (R ₂) (34), vC—C (R ₁) (21), vC—C (R ₂) (12)	
886	7.87	7.55	877	6.88	8.83	–	883	δCH ₂ (R ₂) (37)	
873	10.41	7.49	872	6.20	1.93	–	–	γCH (R ₁) (71) τC—C—C—C (R ₁) (12)	
871	9.89	0.11	867	6.14	6.51	868	–	δCH ₂ (47), τR ₄ (22), vC—O (10)	
857	0.30	2.42	850	0.63	0.84	–	–	δCH ₂ (R ₂) (41), τCH ₂ (R ₄) (16), δCH ₂ (R ₄) (15)	
842	3.36	0.51	833	5.00	0.33	825	830	δCH ₂ (55)	
821	39.98	1.17	814	0.84	0.54	–	–	γCH (R ₁) (97)	
811	0.21	4.64	809	32.08	1.82	–	–	δCH ₂ (34), δR ₄ (15), δC—O (11)	
797	19.14	4.46	789	21.26	6.72	786	792	δCH ₂ (R ₂) (43), τR ₃ (22), γC=O (10)	
756	20.59	0.76	752	88.15	0.36	754	–	γCH (R ₁) (58), τC—C—C—C (R ₁) (29), γC ₅₂ —N ₄₇ (19)	
752	55.24	0.51	750	15.37	1.11	–	–	δCH ₂ (52)	
750	14.62	7.17	743	14.86	7.31	–	738	τR ₄ (13), vC ₄₆ —N ₄₇ (R ₂) (47), vC ₃₁ —N ₃₈ (10)	
724	8.59	3.60	712	14.13	3.17	712	–	δC=O (21), δCH ₂ (19), δR ₄ (12)	
715	0.69	13.58	701	5.17	16.20	–	–	τCN (R ₂) (27), δC—C—C (R ₁) (20)	
707	11.75	5.32	699	7.08	5.01	–	696	τR ₃ (12), γC=O (12)	
692	23.28	1.00	689	38.36	0.02	–	–	τC—C—C—C (R ₁) (82), γCH (R ₁) (28)	
688	2.67	1.33	681	1.47	1.27	681	680	τR ₄ (20), γC=O (16), vC ₆ —C ₇ (15)	
675	26.64	3.48	666	25.54	4.58	–	661	vC—Cl (64), vC—O—C (23)	
655	36.33	3.29	646	34.90	3.07	642	643	vC—Cl (54), δR ₃ (32)	
625	0.11	3.51	610	0.34	5.19	620	624	vC—Cl (42), δC—C—C (R ₁) (21)	
616	8.89	3.47	609	8.87	4.30	–	604	vC—Cl (59), δC—O—C (28)	
611	0.73	3.27	598	1.66	4.82	–	598	δR ₂ (43), δCH ₂ (R ₂) (28), δR ₃ (21)	
600	1.37	6.92	589	1.96	6.02	–	–	δR ₃ (65), δR ₂ (11)	
595	19.53	0.16	588	12.91	0.66	–	572	δC—Cl (51), vC—Cl (15)	
550	0.07	1.91	539	0.05	1.26	–	537	γC—Cl (56), τR ₄ (20), δC=O (12)	
536	6.59	1.61	523	6.94	2.56	–	–	δR ₂ (38), δCH ₂ (24), δC—C—C (R ₁) (13)	
528	19.82	5.63	521	20.78	5.27	–	520	δCH ₂ (32), γC ₁₉ —N ₁₅ (20)	
517	7.02	0.31	510	14.33	0.14	–	500	τC—C—C—C (R ₁) (40), γC ₅₂ —N ₄₇ (35)	
491	0.96	0.88	482	0.51	1.07	–	–	γC=O (32), vC—C (26), τR ₄ (15)	
491	8.32	2.86	481	8.95	2.35	–	481	δR ₂ (52)	
443	0.85	1.36	436	0.32	1.63	–	431	δC—N (31), δR ₂ (15)	
434	14.36	1.42	427	13.95	2.00	–	–	δC ₅₂ —N ₄₇ (57)	
422	15.42	1.60	416	14.00	1.28	420	–	τC—C—C—C (R ₁) (56)	
416	0.29	0.46	412	1.23	0.56	–	404	τC—C—C—C (R ₁) (73)	
375	5.17	1.49	368	5.27	1.25	–	–	δC=O (30), δC—O (26), γC—Cl (17)	
363	0.90	2.66	362	2.49	0.54	–	–	γC ₃₁ —N ₃₈ (42), τR ₂ (23)	
356	7.15	10.61	353	6.09	14.78	–	–	vC—Cl (11), δC—O (31)	
337	1.99	2.48	333	1.83	2.63	–	334	vC—Cl (16), δR ₄ (29)	
329	0.89	7.40	325	0.71	7.64	–	–	vC—Cl (19), τR ₄ (35), δC—O (13)	
324	5.57	6.54	321	6.48	6.27	–	–	γC ₁₉ —N ₁₅ (18), δC—O (10)	
318	11.85	1.43	314	11.74	1.65	–	317	δC—O (62)	
314	2.58	1.27	307	3.74	2.09	–	–	τR ₂ (16)	

(continued on next page)

Table 1 (continued)

B3LYP/6-31G*			B3LYP/SDD IR			Raman		Assignments ^a	
ν	IR _I	R _A	ν	IR _I	R _A	ν	ν		
303	8.13	1.04	299	8.70	0.96	—	—	δ C—O (46)	
282	1.57	2.94	278	2.27	3.01	—	—	δ C ₁₉ —N ₁₅ (43), δ C=O (29)	
278	11.61	4.62	269	15.06	4.31	—	—	τ R ₂ (37)	
270	0.88	2.53	266	3.98	3.93	—	267	δ C ₁₉ —N ₁₅ (17), δ C—Cl (15), δ R ₄ (13)	
269	13.77	3.08	256	3.77	1.34	—	—	τ R ₂ (42), τ C—C—C (R ₁) (11)	
250	2.43	1.22	245	2.08	1.44	—	250	τ C—C—C—C (R ₁) (9), γ C ₃₁ —N ₃₈ (8)	
207	5.51	1.40	203	6.83	1.31	—	—	τ C—O (14), γ C ₁₉ —N ₁₅ (9)	
196	7.39	1.18	193	6.54	1.21	—	—	τ R ₂ (33), τ C—C—C (R ₁) (17), γ C ₃₁ —N ₃₈ (10)	
192	1.34	1.27	188	1.96	1.42	—	—	τ C—O (26), τ R ₃ (12)	
186	0.76	0.46	177	0.41	0.33	—	—	δ C—Cl (20), τ CH ₃ (17)	
179	0.64	0.52	175	0.95	0.36	—	—	τ CH ₃ (30), δ C—Cl (20)	
172	0.97	1.11	169	0.70	1.01	—	167	τ C—O (32)	
160	0.66	1.64	156	0.56	1.43	—	—	δ C—Cl (60)	
159	0.02	3.17	155	0.06	3.70	—	—	δ C—Cl (77)	
157	2.10	0.62	154	1.54	0.78	—	—	τ C—O (21), τ CH ₃ (21)	
152	0.07	0.76	150	0.03	0.92	—	—	δ C—Cl (13), τ CH ₃ (12), τ C—O (11)	
147	1.61	0.47	143	0.99	0.92	—	—	τ C—O (25), δ C—Cl (18)	
140	2.22	2.13	136	3.80	1.43	—	—	τ C—O (33), δ C—O (21), τ CH ₃ (11)	
131	3.19	0.21	129	3.01	0.36	—	—	τ C—O (27)	
124	0.95	0.88	119	0.90	0.73	—	—	τ C—O (29), δ C—O (28)	
119	1.19	0.91	117	1.12	0.67	—	—	τ R ₂ (28), γ C ₃₁ —N ₃₈ (12)	
113	1.02	0.50	112	0.32	0.40	—	—	τ CH ₂ (28), τ R ₂ (32)	
106	0.10	0.63	109	1.29	0.47	—	—	τ R ₃ (47), γ C ₁₉ —N ₁₅ (10)	
86	4.34	0.69	84	4.16	0.49	—	87	τ C—O (36)	
81	0.72	1.15	81	1.42	2.43	—	—	τ R ₃ (53), τ R ₂ (13)	
80	0.61	4.05	79	0.18	2.31	—	—	τ R ₄ (38), γ C—Cl (14), τ R ₂ (12)	
71	0.44	2.05	70	0.66	1.87	—	—	τ C—O (16), γ C ₅₂ —N ₄₇ (12), γ C—Cl (11)	
62	0.13	1.40	60	0.41	0.86	—	—	γ C—Cl (27), τ R ₃ (16), τ R ₄ (15)	
57	0.31	1.00	54	0.40	0.93	—	—	τ R ₃ (33), τ R ₄ (31)	
37	0.01	2.69	34	0.01	2.74	—	—	τ CH ₂ (24), γ C ₅₂ —N ₄₇ (23), τ R ₃ (12)	
23	0.14	2.69	22	0.19	1.69	—	—	τ CH ₂ (27), τ C ₁₉ —N ₁₅ (19), τ R ₂ (18)	
21	0.09	4.46	14	0.08	3.36	—	—	τ CH ₂ (37), τ R ₂ (22)	
11	0.08	1.31	9	0.07	1.39	—	—	τ CH ₂ (53), τ R ₂ (17)	
6	0.18	1.64	7	0.20	1.58	—	—	τ R ₂ (45)	

ν – Stretching; δ – in-plane deformation; γ – out-of-plane deformation; τ – torsion; as – asymmetric; s – symmetric; Phenyl ring – R1; piperazine ring – R2; imido fragment ring – R3; cyclohexene ring – R4; potential energy distribution is given in brackets in the assignment column.

1350–1315 cm⁻¹ in the infrared and more distinctive in Raman spectrum. For the title compound the SDD calculations give the ν CH modes at 3013 and 3002 cm⁻¹. Tarabara et al. [47] and Kas'yan et al. [51] reported the ν CH modes at 3080 cm⁻¹ and 3070–3050 cm⁻¹ for similar derivatives. Atroshchenko et al. [53] reported the CH stretching vibrations at 1805, 1887, 1925, 2968 cm⁻¹ and deformations bands of CH at 1474, 1483 cm⁻¹ theoretically. The deformation bands of the CH are observed at 1281, 1270 cm⁻¹ theoretically for the title compound. Most of the bands are not pure, but contains significant contributions from other modes. For the title compound, the C–C stretching modes are observed at 1093, 1081, 1062, 1054, 1011, 995, 966, 962 cm⁻¹ theoretically and at 1011, 999, 964 cm⁻¹ in the Raman spectrum for the C–C bonds in R3 and R4 and these modes contain contributions from other modes as well.

The vibrations belonging to the bond between the ring and chlorine atoms are worth to discuss here since mixing of vibrations is possible due to the lowering of the molecular symmetry and the presence of heavy atoms on the periphery of the molecule [54–56]. Mooney assigned vibrations of C—Cl, Br and I in the wavenumber range of 1129–480 cm⁻¹ [55,56]. The CCl stretching vibrations give generally strong bands in the region 710–505 cm⁻¹. For simple organic chlorine compounds, CCl absorptions are in the region 750–700 cm⁻¹. Sundaraganesan et al. [57] reported CCl stretching at 704 (IR), 705 (Raman), and 715 cm⁻¹ (DFT) and the deformation bands at 250 and 160 cm⁻¹. The aliphatic CCl bands absorb [38] at 830–560 cm⁻¹ and putting more than one chlorine on a carbon atom raises the CCl wavenumber. The CCl₂ stretching mode is reported at around 738 cm⁻¹ for dichloromethane and scissoring mode δ CCl₂

at around 284 cm⁻¹ [39,40]. Pazdera et al. [58,59] reported the CCl stretching mode at 890 cm⁻¹. For 2-cyanophenylisocyanide dichloride, the CCl stretching mode is reported at 870 (IR), 877 cm⁻¹ (Raman), and 882 cm⁻¹ theoretically [60]. Arslan et al. [61] reported the CCl stretching mode at 683 (experimental) and at 711, 736, 687, and 697 cm⁻¹ theoretically. The deformation bands of CCl are reported [60] at 431, 435, 441, and 441 cm⁻¹. For the title compound, the bands at 642, 620 cm⁻¹ in the IR, 661, 643, 624, 604 cm⁻¹ in Raman and 666, 646, 610, 609 cm⁻¹ (SDD) are assigned as CCl stretching modes. The deformation bands of CCl are also identified. This is in agreement with the literature data [39,62,63]. For 4-chlorophenylboronic acid, the CCl stretching and deformation bands are reported at 571 (DFT), and at 287 and 236 cm⁻¹, respectively [64].

The C=C stretching mode is expected in the region [50] 1667–1640 cm⁻¹. For the title compound, the C=C stretching mode is assigned at 1589 cm⁻¹ in the IR spectrum and at 1594 cm⁻¹ theoretically. For a series of propenoic acid esters, Felfoldi et al. [65] reported the ν C=O at 1690 cm⁻¹ and ν C=C at 1625 cm⁻¹.

El-Emam et al. [66] reported the asymmetric stretching CH₂ vibrations in the piperazine ring in the range 3033–2966 cm⁻¹, while the symmetric vibrations lying in the range 2874–2834 cm⁻¹. For the title compound the bands observed at 2980, 2972, 2968, 2957 cm⁻¹ (SDD) were assigned for CH₂ asymmetric stretching modes. Bands observed at 2921, 2884, 2870, 2822 cm⁻¹ (SDD), 2873, 2831 cm⁻¹ (IR) and 2902, 2878, 2822 cm⁻¹ are assigned for symmetric CH₂ stretching modes for the title compound. In a study on the determination of piperazine rings in ethyleneamines, poly(ethyleneamine) and polyethylenimine by infrared spectrometry, Spell reported that the piperazine ring was found to be

associated with sharp, well-defined absorptions at 1300–1345 cm⁻¹, 1125–1170 cm⁻¹, 1010–1025 cm⁻¹ and 915–940 cm⁻¹ regions of the IR spectrum [67]. El-Emam et al. [66] reported the vibrations of CH₂ groups in the piperazine ring (the asymmetric stretch ν_{as} CH₂, symmetric stretch ν_s CH₂, the scissoring vibration and wagging vibration) in the range 3033–2966, 2874–2834, 1457–1422 and 1379–1344 cm⁻¹ respectively. A very sharp and intense band was observed at 1037 cm⁻¹ by da Silva et al. and was assigned to the ring CH₂ rocking motions. As stated by Spell, [67] this is one of the most useful bands for detecting the presence of di-substituted piperazines. The twisting and rocking vibrations of the CH₂ group appear in the region [38] of 1200–1280 and 740–900 cm⁻¹, respectively. These modes are also assigned (Table 1). For the title compound the twisting vibrations are observed at 1259, 1217 cm⁻¹ in the IR spectrum, 1264, 1226 cm⁻¹ in the Raman spectrum and at 1274, 1255, 1220, 1213 cm⁻¹ theoretically. The rocking deformations are observed at 786 cm⁻¹ in the IR spectrum, 863, 792 cm⁻¹ in the Raman spectrum and at 915, 877, 850, 789 cm⁻¹ theoretically and these modes are not pure, but contain significant contributions from other modes also. El-Emam et al. [66] reported the C–N stretching vibrations in the region 1154–756 cm⁻¹. For the title compound C–N stretching vibrations (C₄₀–N₃₈, C₃₉–N₃₈, C₄₅–N₄₇, C₄₆–N₄₇) are found at 1165, 1096, 905 cm⁻¹ in the IR spectrum, 1166, 1096, 906, 738 cm⁻¹ in the Raman spectrum and at 1161, 1099, 903, 743 cm⁻¹ theoretically. Two absorptions characteristic for the piperazine ring, at 1130 and 1168 cm⁻¹ and assigned for the C–N stretching vibrational modes were observed by da Silva et al. [68]. The shift in the wavenumber may be attributed to the bulky groups attached to the piperazine ring. The C–C stretching vibrations in the piperazine ring were reported at 972, 903 cm⁻¹ [66]. For the title compound these vibrations are observed at 1031, 926 cm⁻¹ theoretically, at 936 cm⁻¹ in IR and at 1021, 928 cm⁻¹ in Raman spectrum.

Geometrical parameters

To the best of our knowledge, no X-ray crystallographic data of this molecule has yet been established. However, the theoretical results obtained are almost comparable with the reported structural parameters of the parent molecules. For the imido fragment of the title compound, the SDD calculations give the bond angles, C₁₆–N₁₅–C₁₃, O₁₈–C₁₃–N₁₅, O₁₈–C₁₃–C₄, N₁₅–C₁₃–C₄, C₁₃–C₄–C₅, C₁₃–C₄–H₁₀, C₅–C₄–H₁₀, C₁₆–C₅–H₁₂, C₄–C₅–H₁₂, O₁₇–C₁₆–N₁₅, O₁₇–C₁₆–C₅, N₁₅–C₁₆–C₅, as 113.8°, 124.3°, 127.4°, 108.1°, 104.9°, 107.7°, 113.7°, 107.9°, 113.6°, 124.3°, 127.4°, 108.2°, respectively, whereas the reported values of similar derivatives are 114.7°, 124.0°, 128.5°, 107.4°, 105.8°, 112.3°, 113.8°, 113.3°, 113.1°, 126.3°, 129.2°, 106.5° and 111.0°, 126.1°, 128.4°, 105.5°, 109.9°, 115.0°, 136.0°, 118.0°, 118.0°, 123.7°, 131.4°, 104.9° [69]. Conley et al. [69] reported the dihedral angles, C₁₆–N₁₅–C₁₃–O₁₈ = 179.5°, C₁₆–N₁₅–C₁₃–C₄ = -4.0°, O₁₈–C₁₃–C₄–C₅ = 177.5°, N₁₅–C₁₃–C₄–C₅ = -0.5°, C₁₃–C₄–C₅–C₁₆ = 1.7°, C₁₃–N₁₅–C₁₆–C₅ = 5.1°, C₄–C₅–C₁₆–O₁₇ = 176.7°, C₄–C₅–C₁₆–N₁₅ = -4.0° whereas for the title compound the corresponding values are 178.7°, -6.2°, 176.4°, 1.5°, 2.9°, 8.2°, 177.6° and -6.5° respectively. Pinho e Melo et al. [70] reported the bond lengths N₁₅–C₁₆ = 1.3654, N₁₅–C₁₃ = 1.4484 Å, bond angles C₁₆–N₁₅–C₁₃ = 116.8°, C₁₆–N₁₅–C₁₉ = 121.6°, C₁₃–N₁₅–C₁₉ = 121.6°, C₅–C₁₆–N₁₅ = 121.9°, N₁₅–C₁₃–C₄ = 107° and dihedral angles C₁₃–N₁₅–C₁₆–C₅ = 177.2°, C₁₆–N₁₅–C₁₃–C₄ = 169.9° which are in agreement with our calculated values.

Lee and Swager [71] reported the bond lengths O₁₇–C₁₆ = 1.1954, O₁₈–C₁₃ = 1.2054, N₁₅–C₁₆ = 1.3776, N₁₅–C₁₃ = 1.3765 Å and the bond angles C₅–C₁₆–N₁₅ = 106.3°, C₄–C₁₃–N₁₅ = 106.5°. The B3LYP calculations give the bond lengths within the imido fragment as C₁₆–O₁₇ = 1.2426, N₁₅–C₁₆ = 1.4021, C₁₃–O₁₈ = 1.2409, C₁₃–N₁₅ = 1.4037, C₁₃–C₄ = 1.5346, C₁₆–C₅ = 1.5391,

C₅–C₄ = 1.5693 Å. Conley et al. [69] reported the corresponding values as 1.2025, 1.3985, 1.2104, 1.4054, 1.4865, 1.5155, 1.555 Å and 1.1974, 1.3995, 1.2004, 1.3824, 1.4866, 1.4826, 1.3436 Å for different similar derivatives. The N₁₅–C₁₉ bond length (1.4729 Å) is longer than N₁₅–C₁₃ (1.4037 Å) and N₁₅–C₁₆ (1.4021 Å) bond lengths. This indicates, as expected, a delocalized π-electron system along the imide part of the molecule (O₁₈–C₁₃–N₁₅–C₉–O₁₇) as reported by Bartkowska et al. [72]. Bartkowska et al. [72] reported the bond lengths, C₁₃–O₁₈ = 1.2032, N₁₅–C₁₃ = 1.3913, C₁₃–C₄ = 1.5193, C₄–C₅ = 1.5453, C₁₆–O₁₇ = 1.2073, N₁₅–C₁₆ = 1.388 Å and the bond angles, N₁₅–C₁₉–C₂₈ = 111.3°, O₁₈–C₁₃–N₁₅ = 124.3°, O₁₈–C₁₃–C₄ = 127.8°, N₁₅–C₁₃–C₄ = 107.8°, O₁₇–C₁₆–N₁₅ = 127.2°, N₁₅–C₁₆–C₅ = 107.0°, C₁₆–N₁₅–C₁₃ = 114.2°, C₁₆–N₁₅–C₁₉ = 123.8°, C₁₃–N₁₅–C₁₉ = 121.7°, whereas the corresponding values in the present case are 1.2409, 1.4037, 1.5346, 1.5693, 1.2426, 1.4021 Å and 112.7°, 124.3°, 127.4°, 108.1°, 124.3°, 108.2°, 113.8°, 123.5°, 122.6°.

For the title compound the C₄–H₁₀, C₅–H₁₂, bond lengths are 1.0936, 1.0939 Å whereas reported values are 0.96, 0.9601 Å [69]. The cyclohexene ring fragment is a sterically strained system. Presumably, this is the reason for elongation of skeletal C–C bonds, C₁–C₂, C₂–C₃, C₃–C₄, C₅–C₆, C₆–C₁. The C–C bond lengths in the five member ring (C₅–C₁₆, C₄–C₁₃) are elongated to a lesser extent. These may be explained by change of the substitution pattern in the nitrogen containing five member ring as reported by Tarabara et al. [47].

The methoxy groups, O₁₄–C₁₁–H_{23,24,27} and O₉–C₈–H_{20,21,22} inclined almost equally with respect to the other parts of the six member ring. The bond angles C₁–C₆–C₇, C₅–C₆–C₇, C₂–C₃–C₇, C₄–C₃–C₇, C₆–C₁–C₂ and C₄–C₃–C₂ are respectively 99.7°, 102.1°, 99.7°, 102.8°, 107.8° and 105.2°. In addition the declination of the five member ring from the cyclohexene ring are given by the angles C₆–C₅–C₁₆ and C₃–C₄–C₁₃ by 118.7° and 119.2° which are almost equal as reported in the literature [47]. The conjugation in the imido group is essentially disturbed; the torsion angles C₁₃–N₁₅–C₁₆–C₅, C₁₆–N₁₅–C₁₃–C₄ are 8.2°, -6.2° and the C₁₃–N₁₅ and C₁₆–N₁₅ bond lengths are elongated to 1.4037, 1.4021 Å relative to the average value 1.371 Å [73].

For the cyclohexene ring, Manohar et al. [74] reported the bond lengths C₁–C₂ = 1.3194, C₁–C₆ = 1.5174, C₆–C₅ = 1.5523, C₆–C₇ = 1.5484, C₅–C₄ = 1.5353, C₄–C₃ = 1.5543, C₃–C₇ = 1.5473, C₃–C₂ = 1.5144 Å and the corresponding bond lengths of the title compound are 1.3472, 1.5334, 1.5705, 1.5870, 1.5693, 1.5750, 1.5903, 1.5311 Å. The bond angles reported by Manohar et al. [74] are C₃–C₄–C₅ = 102.9°, C₃–C₂–C₁ = 107.5°, C₃–C₇–C₆ = 92.4°, C₂–C₃–C₄ = 107.2°, C₆–C₅–C₄ = 103.1°, C₆–C₁–C₂ = 107.7°, C₅–C₆–C₁ = 106.8°, C₂–C₃–C₇ = 99.52°, C₄–C₃–C₇ = 101.12°, C₅–C₆–C₇ = 101.1°, C₁–C₆–C₇ = 99.4°, where as the corresponding calculated (SDD) values of the title compound are 102.8°, 107.4°, 91.3°, 105.2°, 102.9°, 107.8°, 106.1°, 99.7°, 102.8°, 102.1°, 99.7°.

In the present case, the oxygen atoms O₁₇ and O₁₈ are equally inclined from the N₁₅ atom given by the angles O₁₇–C₁₆–N₁₅, O₁₈–C₁₃–N₁₅ (124.3°) and from C₄ and C₅ atoms given by the angles O₁₇–C₁₆–C₅, O₁₈–C₁₃–C₄ (127.4°) as reported in the literature [75].

There are four types of CC bonds involved in the title compound, strained CC bonds of R1, R2, R3, R4, propyl group and of the carbon–carbon bridge. The CC bond lengths are in the range 1.5346–1.5693, 1.5311–1.5750, 1.5415–1.5432 Å, in R3, R4, propyl group and 1.5903, 1.5870 Å in the carbon–carbon bridge respectively. The CH bond lengths are C₄–H₁₀ = 1.0936 and C₅–H₁₂ = 1.0939 Å. The CH bond lengths are in the range 1.0958–1.1119 Å for the bridging CH₂ groups, and for the CH₃ groups, CH bond lengths are in the range of 1.0918–1.0951 Å. The optimized carbon–carbon bridge angles C₃–C₇–C₆ = 91.3° is similar to the structures reported by Manohar et al. [74].

The propyl group is tilted from the R2, as is evident from torsion angles, C₅—C₁₆—N₁₅—C₁₉ (-176.4°), C₁₆—N₁₅—C₁₉—C₂₈ (-92.8°), C₄—C₁₃—N₁₅—C₁₉ (178.4°) and C₁₃—N₁₅—C₁₉—C₂₈ (82.2°). The double bonds C₁₆—O₁₇ and C₁₃—O₁₈ are conjugated with the π -system of the R3, with the torsion angles O₁₇—C₁₆—N₁₅—C₁₃, C₁₆—N₁₅—C₁₃—C₄ being -175.8° , -6.2° and O₁₈—C₁₃—N₁₅—C₁₆, C₁₃—N₁₅—C₁₆—C₅ being 178.7° , 8.2° respectively as reported by Kasyan et al. [76]. At N₁₅ position, the bond angles C₁₆—N₁₅—C₁₉ = 123.5° , C₁₃—N₁₅—C₁₉ = 122.6° and C₁₆—N₁₅—C₁₃ = 113.8° and this asymmetry of angles reveal the steric repulsion of the atoms H₂₆, H₂₅ and O₁₇, O₁₈ [76].

For the piperazine ring, El-Emam et al. [66] reported the bond lengths N₃₈—C₄₀ = 1.465, N₃₈—C₃₉ = 1.463, C₃₉—C₄₆ = 1.514, N₄₇—C₄₅ = 1.458, N₄₇—C₄₆ = 1.471, C₄₀—C₄₅ = 1.511 and the corresponding bond lengths of the title compound are 1.4887, 1.4799, 1.5362, 1.4722, 1.4742, 1.5453 Å respectively. The B3LYP calculations give the bond angles within the piperazine ring N₃₈—C₃₉—C₄₆ = 111.2° , N₃₈—C₄₀—C₄₅ = 113.6° , N₄₇—C₄₅—C₄₀ = 110.3° , N₄₇—C₄₆—C₃₉ = 110.4° , C₄₅—N₄₇—C₄₆ = 116.8° . El-Emam et al. [66] reported the corresponding values as 110.0° , 109.7° , 109.7° , 110.0° and 110.0° for different similar derivatives. Karczmarzyk et al. [77] reported the dihedral angles C₄₀—N₃₈—C₃₉—C₄₆ = 61.1° , C₄₅—N₄₇—C₄₆—C₃₉ = 60.1° , N₃₈—C₃₉—C₄₆—N₄₇ = -61.5° , C₄₆—N₄₇—C₄₅—C₄₀ = -58.2° , C₃₉—N₃₈—C₄₀—C₄₅ = -58.9° , N₄₇—C₄₅—C₄₀—N₃₈ = 57.5° , which are in agreement with our calculated values.

First hyperpolarizability

Non-linear optics deals with the interaction of applied electromagnetic fields in various materials to generate new electromagnetic fields, altered in wavenumber, phase, or other physical properties [78]. Organic molecules able to manipulate photonic signals efficiently are of importance in technologies such as optical communication, optical computing, and dynamic image processing [79,80]. In this context, the dynamic first hyperpolarizability of the title compound is also calculated in the present study. The first hyperpolarizability (β_0) of this novel molecular system is calculated using SDD method, based on the finite field approach. In the presence of an applied electric field, the energy of a system is a function of the electric field. First hyperpolarizability is a third rank tensor that can be described by a $3 \times 3 \times 3$ matrix. The 27 components of the 3D matrix can be reduced to 10 components due to the Kleinman symmetry [81]. The components of β are defined as the coefficients in the Taylor series expansion of the energy in the external electric field. When the electric field is weak and homogeneous, this expansion becomes

$$E = E_0 - \sum_i \mu_i F^i - \frac{1}{2} \sum_{ij} \alpha_{ij} F^i F^j - \frac{1}{6} \sum_{ijk} \beta_{ijk} F^i F^j F^k - \frac{1}{24} \sum_{ijkl} \gamma_{ijkl} F^i F^j F^k F^l + \dots$$

where E_0 is the energy of the unperturbed molecule, F_i is the field at the origin, μ_{ij} , α_{ij} , β_{ijk} and γ_{ijkl} are the components of dipole moment, polarizability, the first hyperpolarizabilities, and second hyperpolarizabilities, respectively. The calculated first hyperpolarizability of the title compound is 4.49×10^{-30} esu, which comparable with the reported values of similar derivatives [82] and which is 34.54 times that of the standard NLO material urea (0.13×10^{-30} esu) [83]. Panicker et al. [26] and Varghese et al. [27] reported the first hyperpolarizability of similar azatricyclo derivatives as 0.55×10^{-30} and 0.89×10^{-30} esu. We conclude that the title compound is an attractive object for future studies of non-linear optical properties.

NBO analysis

The natural bond orbital (NBO) calculations were performed using NBO 3.1 program [84] as implemented in the Gaussian09

package at the DFT/B3LYP level in order to understand various second-order interactions between the filled orbital of one subsystem and vacant orbital of another subsystem, which is a measure of the intermolecular delocalization or hyper conjugation. NBO analysis provides the most accurate possible ‘natural Lewis structure’ picture of ‘j’ because all orbital details are mathematically chosen to include the highest possible percentage of the electron density. A useful aspect of the NBO method is that it gives information about interactions of both filled and virtual orbital spaces that could enhance the analysis of intra and inter molecular interactions. The second-order Fock-matrix was carried out to evaluate the donor-acceptor interactions in the NBO basis. The interactions result in a loss of occupancy from the localized NBO of the idealized Lewis structure into an empty non-Lewis orbital. For each donor (i) and acceptor (j) the stabilization energy ($E2$) associated with the delocalization i → j is determined as

$$E(2) = \Delta E_{ij} = q_i \frac{(F_{ij})^2}{(E_j - E_i)}$$

where q_i is the donor orbital occupancy, E_i , E_j the diagonal elements, and F_{ij} is the off diagonal NBO Fock matrix element.

In NBO analysis large $E(2)$ value shows the intensive interaction between electron donors and electron-acceptors, and greater the extent of conjugation of the whole system, the possible intensive interaction are given in Table S2 as Supporting material. The second order perturbation theory analysis of Fock-matrix in NBO basis shows strong intermolecular hyper conjugative interactions are formed by orbital overlap between n(O) and $\sigma^*(C=O)$, $\sigma^*(C-C)$, $\sigma^*(C-N)$, n(N) and $\pi^*(C=C)$ and between n(Cl) and $\pi^*(C=C)$ bond orbitals which result in ICT causing stabilization of the system. These interactions are observed as an increase in electron density (ED) in C—O, C—C and C—N anti bonding orbital that weakens the respective bonds. There occurs a strong inter molecular hyper conjugative interaction of C₇—O₁₄ from O₉ of n₂(O₉) → $\sigma^*(C_7-O_{14})$ which increases ED (0.07306 e) that weakens the respective bonds C₇—O₁₄ (1.4229 Å) leading to stabilization of 12.60 kJ/mol and also the hyper conjugative interaction of N₁₅—C₁₆ from O₁₇ of n₂(O₁₇) → $\sigma^*(N_{15}-C_{16})$ which increases ED (0.08760 e) that weakens the respective bonds N₁₅—C₁₆ (1.4021 Å) leading to stabilization of 26.17 kJ/mol. Also the hyper conjugative interaction of C₁₃—N₁₅ from O₁₈ of n₂(O₁₈) → $\sigma^*(C_{13}-N_{15})$ which increases ED (0.08859 e) that weakens the respective bonds C₁₃—N₁₅ (1.4037 Å) leading to stabilization of 26.17 kJ/mol. An another hyper conjugative interaction observed in C₁₆—O₁₇ from N₁₅ of n₁(N₁₅) → $\pi^*(C_{16}-O_{17})$ which increases ED (0.24591 e) that weakens the respective bond C₁₆—O₁₇ (1.2426 Å) leading to a stabilization of 55.22 kJ/mol. An another hyper conjugative interaction observed in C₃—C₇ from Cl₃₄ of n₃(Cl₃₄) → $\sigma^*(C_3-C_7)$ which increases ED (0.08303 e) that weakens the respective bond C₃—C₇ (1.5903 Å) leading to a stabilization of 5.10 kJ/mol. Another hyper conjugative interaction is observed C₁—C₂ from Cl₃₅ of n₃(Cl₃₅) → $\pi^*(C_1-C_2)$ which increases ED (0.19679 e) that weakens the respective bonds C₁—C₂ (1.3472 Å) leading to stabilization of 14.59 kJ/mol. There occurs another strong intermolecular hyper conjugative interaction of C₁—C₂ from Cl₃₆ of n₃(Cl₃₆) → $\pi^*(C_1-C_2)$ which increases ED (0.19679 e) that weakens the respective bonds C₁—C₂ (1.3472 Å) leading to stabilization of 14.89 kJ/mol. Another hyper conjugative interaction of C₆—C₇ from Cl₃₇ of n₃(Cl₃₇) → $\sigma^*(C_6-C_7)$ which increases ED (0.08183 e) that weakens the respective bond C₆—C₇ (1.5870 Å) leading to a stabilization of 4.54 kJ/mol. Also the hyper conjugative interaction of C₄₀—C₄₅ from N₃₈ of n₁(N₃₈) → $\sigma^*(C_{40}-C_{45})$ which increases ED (0.02217 e) that weakens the respective bonds C₄₀—C₄₅ (1.5453 Å) leading to stabilization of 4.29 kJ/mol. There occurs another strong intermolecular hyper conjugative

interaction of C₅₂—C₅₄ from N₄₇ of n₁(N₄₇) → π*(C₅₂—C₅₄) which increases ED (0.43183 e) that weakens the respective bonds C₅₂—C₅₄ (1.4251 Å) leading to stabilization of 41.0 kJ/mol. These interactions are observed as an increase in electron density (ED) in C—O, C—C and C—N anti bonding orbital that weakens the respective bonds.

The increased electron density at the oxygen atoms leads to the elongation of respective bond length and a lowering of the corresponding stretching wavenumber. The electron density (ED) is transferred from the n(O) to the anti-bonding π* orbital of the C—O, C—C and C—N bonds, explaining both the elongation and the red shift [85]. The hyper conjugative interaction energy was deduced from the second-order perturbation approach. Delocalization of electron density between occupied Lewis-type (bond or lone pair) NBO orbital and formally unoccupied (anti bond or Rydberg) non-Lewis NBO orbital corresponds to a stabilizing donor–acceptor interaction. The OCH₃ and C=O, C—Cl stretching modes can be used as a good probe for evaluating the bonding configuration around the ring. Hence the title compound is stabilized by these orbital interactions.

The NBO analysis also describes the bonding in terms of the natural hybrid orbital n₂(O₉), which occupy a higher energy orbital (−0.32194 a.u.) with considerable p-character (99.80%) and low occupation number (1.90187) and the other n₁(O₉), which occupy a lower energy orbital (−0.57322 a.u.) with considerable p-character (56.05%) and high occupation number (1.95769). Also n₂(O₁₄), which occupy a higher energy orbital (−0.32774 a.u.) with considerable p-character (100.0%) and low occupation number (1.90180) and the other n₁(O₁₄), which occupy a lower energy orbital (−0.58495 a.u.) with considerable p-character (55.98%) and high occupation number (1.95485). Again n₂(O₁₇), which occupy a higher energy orbital (−0.27654 a.u.) with considerable p-character (99.99%) and low occupation number (1.86035) and the other n₁(O₁₇), which occupy a lower energy orbital (−0.70945 a.u.) with considerable p-character (38.34%) and high occupation number (1.97607). Again n₂(O₁₈), which occupy a higher energy orbital (−0.27433 a.u.) with considerable p-character (99.99%) and low occupation number (1.85991) and the other n₁(O₁₈), which occupy a lower energy orbital (−0.70651) with considerable p-character (38.43%) and high occupation number (1.97646). Again n₃(Cl₃₄), which occupy a high energy orbital (−0.32748 a.u.) with considerable p-character (100.0%) and low occupation number (1.96154) and the other n₂(Cl₃₄) which occupy a low energy orbital (−0.32931 a.u.) with considerable p-character (99.99%) and high occupation number (1.96588). Another n₃(Cl₃₅), which occupy a high energy orbital (−0.34372 a.u.) with considerable p-character (100.0%) and low occupation number (1.91960) and the other n₂(Cl₃₅), which occupies a low energy orbital (−0.34463 a.u.) with considerable p-character (99.87%) and high occupation number (1.96363). Another n₃(Cl₃₆), which occupy a energy orbital (−0.34164 a.u.) with considerable p-character (100.0%) and low occupation number (1.91712) and the other n₂(Cl₃₆), which occupy a low energy orbital (−0.34301 a.u.) with considerable p-character (99.86%) and high occupation number (1.96325). Another n₃(Cl₃₇), which occupy a high energy orbital (−0.32349 a.u.) with considerable p-character (100.0%) and low occupation number (1.96083) and the other n₂(Cl₃₇) which occupy a low energy orbital (−0.32654 a.u.) with considerable p-character (99.97%) and high occupation number (1.96571). Thus, a very close to pure p-type lone pair orbital participates in the electron donation to the σ*(C—O), σ*(N—C) and σ*(C—C) orbital for n₃(O₉) → σ*(C—O), n₃(O₁₈) → σ*N₁₅—C₁₃ and n₁(N₄₇) → σ*C₅₂—C₅₄ interactions respectively in the compound. The results are tabulated in Table 2.

Mulliken charges

Mulliken charges are calculated by determining the electron population of each atom as defined in the basis functions. The

charge distributions calculated by the Mulliken [86] and NBO methods for the equilibrium geometry of TDPPAD are given in Table S3 as Supporting material. The charge distribution on the molecule has an important influence on the vibrational spectra. In TDPPAD, the Mulliken atomic charge of the carbon atoms in the neighborhood of C₇, C₁₃, C₁₆ and C₅₂ become more positive, shows the direction of delocalization and shows that the natural atomic charges are more sensitive to the changes in the molecular structure than Mulliken's net charges. The results are shown in Fig. S1 as Supporting material.

Also we done a comparison of Mulliken charges obtained by different basis sets and tabulated in Table S4 as Supporting material in order to assess the sensitivity of the calculated charges to changes in (i) the choice of the basis set and (ii) the choice of the quantum mechanical method. The results can, however, better be represented in graphical form as shown in Fig. S2 as supporting material. We have observed a change in the charge distribution by changing different basis sets.

¹H NMR spectrum

The experimental spectrum data of TDPPAD in DMSO with TMS as internal standard is obtained at 400 MHz. The absolute isotropic chemical shielding of TDPPAD was calculated by B3LYP/GIAO model [87]. Relative chemical shifts were then estimated by using the corresponding TMS shielding: $\delta_{\text{calc}} = \sigma_{\text{calc}} \cdot (\text{TMS}) - \sigma_{\text{calc}}$ together with calculated values of $\sigma_{\text{calc}} \cdot (\text{TMS})$, are given in Table 3. It could be seen from Table 3 that chemical shift was in agreement with the experimental ¹H NMR data. Thus, the results showed that the predicted proton chemical shifts were in good agreement with the experimental data for TDPPAD.

PES scan studies

A detailed potential energy surface (PES) scan on dihedral angles C₃₁—C₂₈—C₁₉—N₁₅ and N₃₈—C₃₁—C₂₈—C₁₉ have been performed at B3LYP/6-31G(d) level to reveal all possible conformations of TDPPAD. The PES scan was carried out by minimizing the potential energy in all geometrical parameters by changing the torsion angle at every 20° for a 180° rotation around the bond. The results obtained in PES scan study by varying the torsion perturbation around the methyl bonds (CH₂) are plotted and given in Figs. 4 and 5. For the C₃₁—C₂₈—C₁₉—N₁₅ rotation, the minimum energy was obtained at −175.5° in the potential energy curve of energy −3209.19188 Hartrees. For the N₃₈—C₃₁—C₂₈—C₁₉ rotation, the minimum energy occurs at 178.3° in the potential energy curve of energy −3209.19257 Hartrees.

Molecular electrostatic potential

MEP is related to the ED and is a very useful descriptor in understanding sites for electrophilic and nucleophilic reactions as well as hydrogen bonding interactions [88,89]. The electrostatic potential V(r) is also well suited for analyzing processes based on the “recognition” of one molecule by another, as in drug-receptor, and enzyme–substrate interactions, because it is through their potentials that the two species first “see” each other [90,91]. To predict reactive sites of electrophilic and nucleophilic attacks for the investigated molecule, MEP at the B3LYP/6-31G(d,p) optimized geometry was calculated. The negative (red and yellow) regions of MEP were related to electrophilic reactivity and the positive (blue) regions to nucleophilic reactivity (Fig. S3 Supporting material). From the MEP it is evident that the negative charge covers the carbonyl, benzene and piperazine rings and the positive region is over the methyl group. The more electro negativity in the carbonyl,

Table 2

NBO results showing the formation of Lewis and non-Lewis orbitals.

Bond (A–B)	ED (e ^{−1})	EDA%	EDB%	NBO	s%	p%
σC ₁ –C ₂	1.97964	49.95	50.05	0.7067 (sp ^{1.53})C	39.56	60.44
–	−0.80470	–	–	+0.7075 (sp ^{1.52})C	39.62	60.38
πC ₁ –C ₂	1.94592	49.58	50.42	0.7041 (sp ^{94.85})C	1.04	98.96
–	−0.36201	–	–	+0.7101 (sp ^{99.99})C	0.97	99.03
σC ₁ –C ₆	1.96243	49.21	50.79	0.7015 (sp ^{1.96})C	33.80	66.20
–	−0.69163	–	–	+0.7126 (sp ^{2.66})C	27.35	72.65
σC ₁ –Cl36	1.98987	47.58	52.42	0.6898 (sp ^{2.93})C	25.43	74.57
–	−0.74647	–	–	+0.7240 (sp ^{5.55})Cl	15.27	84.73
σC ₂ –C ₃	1.96329	49.24	50.76	0.7017 (sp ^{1.96})C	33.80	66.20
–	−0.69347	–	–	+0.7124 (sp ^{2.66})C	27.29	72.71
σC ₂ –Cl35	1.98986	47.53	52.47	0.6894 (sp ^{2.93})C	25.43	74.57
–	−0.74685	–	–	+0.7244 (sp ^{5.56})Cl	15.25	84.75
σC ₃ –C ₄	1.95846	51.20	48.80	0.7156 (sp ^{2.64})C	27.50	72.50
–	−0.65078	–	–	+0.6986 (sp ^{2.95})C	25.32	74.68
σC ₃ –C ₇	1.95153	52.04	47.96	0.7214 (sp ^{2.86})C	25.91	74.09
–	−0.65147	–	–	+0.6925 (sp ^{2.74})C	26.73	73.27
σC ₃ –Cl34	1.98597	47.43	52.57	0.6887 (sp ^{4.27})C	18.97	81.03
–	−0.69288	–	–	+0.7251 (sp ^{6.10})Cl	14.09	85.91
σC ₄ –C ₅	1.95374	49.96	50.04	0.7068 (sp ^{3.17})C	23.95	76.05
–	−0.62402	–	–	+0.7074 (sp ^{3.17})C	23.95	76.05
σC ₄ –C ₁₃	1.97494	52.50	47.50	0.7246 (sp ^{2.93})C	25.47	74.53
–	−0.67254	–	–	+0.6892 (sp ^{1.77})C	36.11	63.89
σC ₅ –C ₆	1.96075	48.97	51.03	0.6998 (sp ^{2.91})C	25.59	74.41
–	−0.65358	–	–	+0.7143 (sp ^{2.64})C	27.47	72.53
σC ₅ –C ₁₆	1.97465	52.34	47.66	0.7235 (sp ^{2.98})C	25.15	74.85
–	−0.67160	–	–	+0.6904 (sp ^{1.77})C	36.09	63.91
σC ₆ –C ₇	1.94980	52.03	47.97	0.7213 (sp ^{2.89})C	25.72	74.28
–	−0.65073	–	–	+0.6926 (sp ^{2.77})C	26.53	73.47
σC ₆ –Cl37	1.98578	47.64	52.36	0.6902 (sp ^{4.23})C	19.12	80.88
–	−0.69161	–	–	+0.7236 (sp ^{6.09})Cl	14.11	85.89
σC ₇ –O ₉	1.99160	33.71	66.29	0.5806 (sp ^{3.23})C	23.66	76.34
–	−0.89957	–	–	+0.8142 (sp ^{2.27})O	30.56	69.44
σC ₇ –O ₁₄	1.99140	33.17	66.83	0.5760 (sp ^{3.38})C	22.82	77.18
–	−0.89458	–	–	+0.8175 (sp ^{2.27})O	30.55	69.45
σC ₈ –O ₉	1.98904	31.41	68.59	0.5605 (sp ^{4.29})C	18.89	81.11
–	−0.78548	–	–	+0.8282 (sp ^{2.96})O	25.28	74.72
σC ₁₁ –O ₁₄	1.98839	30.96	69.04	0.5564 (sp ^{4.42})C	18.45	81.55
–	−0.78449	–	–	+0.8309 (sp ^{2.93})O	25.43	74.57
σC ₁₃ –N ₁₅	1.98547	36.38	63.62	0.6032 (sp ^{2.29})C	30.36	69.64
–	−0.83157	–	–	+0.7976 (sp ^{2.04})N	32.89	67.11
σC ₁₃ –O ₁₈	1.99552	35.28	64.72	0.5940 (sp ^{2.00})C	33.29	66.71
–	−1.08580	–	–	+0.8045 (sp ^{1.61})O	38.37	61.63
πC ₁₃ –O ₁₈	1.98592	32.94	67.06	0.5739 (sp ^{99.99})C	0.01	99.99
–	−0.39079	–	–	+0.8189 (sp ^{99.99})O	0.06	99.94
σN ₁₅ –C ₁₆	1.98586	63.50	36.50	0.7969 (sp ^{2.01})N	33.19	66.81
–	−0.83572	–	–	+0.6041 (sp ^{2.28})C	30.52	69.48
σN ₁₅ –C ₁₉	1.98438	64.15	35.85	0.8009 (sp ^{1.96})N	33.74	66.26
–	−0.75820	–	–	+0.5988 (sp ^{3.72})C	21.20	78.80
σC ₁₆ –O ₁₇	1.99554	35.31	64.69	0.5942 (sp ^{2.02})C	33.09	66.91
–	−1.08481	–	–	+0.8043 (sp ^{1.62})O	38.17	61.83
πC ₁₆ –O ₁₇	1.98594	32.75	67.25	0.5723 (sp ^{99.99})C	0.09	99.91
–	−0.39565	–	–	+0.8201 (sp ^{99.99})O	0.18	99.82
σC ₁₉ –C ₂₈	1.97889	50.98	49.02	0.7140 (sp ^{2.47})C	29.82	71.18
–	−0.60792	–	–	+0.7002 (sp ^{2.88})C	25.74	74.26
σC ₂₈ –C ₃₁	1.98119	50.11	49.89	0.7079 (sp ^{2.75})C	26.67	73.33
–	−0.59944	–	–	+0.7063 (sp ^{2.58})C	27.91	72.09
σC ₃₁ –N ₃₈	1.98472	39.74	60.26	0.6304 (sp ^{3.17})C	23.98	76.02
–	−0.69946	–	–	+0.7763 (sp ^{2.29})N	30.38	69.62
σN ₃₈ –C ₃₉	1.98587	60.29	39.71	0.7765 (sp ^{2.37})N	29.66	70.34
–	−0.69495	–	–	+0.6302 (sp ^{3.27})C	23.42	76.58
σN ₃₈ –C ₄₀	1.98566	60.27	39.73	0.7763 (sp ^{2.40})N	29.41	70.59
–	−0.68933	–	–	+0.6304 (sp ^{3.32})C	23.15	76.85
σC ₃₉ –C ₄₆	1.98375	49.82	50.18	0.7058 (sp ^{2.67})C	27.23	72.77
–	−0.61073	–	–	+0.7084 (sp ^{2.64})C	27.47	72.53
σC ₄₀ –C ₄₅	1.98673	49.39	50.61	0.7028 (sp ^{2.66})C	27.34	72.66
–	−0.60617	–	–	+0.7114 (sp ^{2.67})C	27.28	72.72
σC ₄₅ –N ₄₇	1.98604	38.41	61.59	0.6197 (sp ^{3.38})C	22.82	77.18
–	−0.71137	–	–	+0.7848 (sp ^{2.15})N	31.77	68.23
σC ₄₆ –N ₄₇	1.98583	38.39	61.61	0.6196 (sp ^{3.39})C	22.76	77.24
–	−0.70934	–	–	+0.7849 (sp ^{2.16})N	31.61	68.39
σN ₄₇ –C ₅₂	1.98642	61.26	38.74	0.7827 (sp ^{1.73})N	36.62	63.38
–	−0.78136	–	–	+0.6224 (sp ^{2.49})C	28.69	71.31
σC ₅₂ –C ₅₃	1.97354	51.17	48.83	0.7153 (sp ^{1.80})C	35.66	64.34
–	−0.67150	–	–	+0.6988 (sp ^{1.94})C	34.04	65.96

Table 2 (continued)

Bond (A–B)	ED (e ^a)	EDA%	EDB%	NBO	s%	p%
σC52–C54	1.97348	51.16	48.84	0.7153 (sp ^{1.81})C	35.59	64.41
–	-0.67112	–	–	+0.6988 (sp ^{1.94})C	34.03	65.97
πC52–C54	1.63395	45.79	54.21	0.6767 (sp ^{1.00})C	0.00	100.0
–	-0.23294	–	–	+0.7363 (sp ^{1.00})C	0.00	100.0
σC53–C55	1.97867	50.39	49.61	0.7099 (sp ^{1.77})C	36.04	63.96
–	-0.67364	–	–	+0.7043 (sp ^{1.84})C	35.18	64.82
πC53–C55	1.72012	53.44	46.56	0.7310 (sp ^{1.00})C	0.00	100.0
–	-0.23368	–	–	+0.6824 (sp ^{1.00})C	0.00	100.0
σC54–C57	1.97870	50.39	49.61	0.7098 (sp ^{1.77})C	36.04	63.96
–	-0.67373	–	–	+0.7044 (sp ^{1.84})C	35.19	64.81
σC55–C59	1.98074	50.27	49.73	0.7090 (sp ^{1.83})C	35.34	64.66
–	-0.66703	–	–	+0.7052 (sp ^{1.88})C	34.73	65.27
σC57–C59	1.98075	50.27	49.73	0.7090 (sp ^{1.83})C	35.34	64.66
–	-0.66702	–	–	+0.7052 (sp ^{1.88})C	34.73	65.27
πC57–C59	1.67792	47.52	52.48	0.6893 (sp ^{1.00})C	0.00	100.0
–	-0.22776	–	–	+0.7244 (sp ^{1.00})C	0.00	100.0
n1O9	1.95769	–	–	sp 1.28	43.95	56.05
–	-0.57322	–	–	–	–	–
n2O9	1.90187	–	–	sp 99.99	0.20	99.80
–	-0.32194	–	–	–	–	–
n1O14	1.95485	–	–	sp 1.27	44.02	55.98
–	-0.58495	–	–	–	–	–
n2 O14	1.90180	–	–	sp 1.00	0.00	100.0
–	-0.32774	–	–	–	–	–
n1 N15	1.58084	–	–	sp 99.99	0.17	99.83
–	-0.28378	–	–	–	–	–
n1 O17	1.97607	–	–	sp 0.62	61.66	38.34
–	-0.70945	–	–	–	–	–
n2 O17	1.86035	–	–	sp 99.99	0.01	99.99
–	-0.27654	–	–	–	–	–
n1 O18	1.97646	–	–	sp 0.62	61.57	38.43
–	-0.70651	–	–	–	–	–
n2 O18	1.85991	–	–	sp 1.00	0.01	99.99
–	-0.27433	–	–	–	–	–
n1Cl34	1.99303	–	–	sp 0.16	86.08	13.92
–	-0.96695	–	–	–	–	–
n2 Cl34	1.96588	–	–	sp 1.00	0.01	99.99
–	-0.32931	–	–	–	–	–
n3 Cl34	1.96154	–	–	sp 1.00	0.00	100.0
–	-0.32748	–	–	–	–	–
n1 Cl35	1.99269	–	–	sp 0.18	84.82	15.18
–	-0.96823	–	–	–	–	–
n2 Cl35	1.96363	–	–	sp 99.99	0.13	99.87
–	-0.34463	–	–	–	–	–
n3 Cl35	1.91960	–	–	sp 1.00	0.00	100.0
–	-0.34372	–	–	–	–	–
n1 Cl36	1.99259	–	–	sp 0.18	84.80	15.20
–	-0.96679	–	–	–	–	–
n2 Cl36	1.96325	–	–	sp 99.99	0.14	99.86
–	-0.34301	–	–	–	–	–
n3 Cl36	1.91712	–	–	sp 1.00	0.00	100.0
–	-0.34164	–	–	–	–	–
n1 Cl37	1.99308	–	–	sp 0.16	86.04	13.96
–	-0.96347	–	–	–	–	–
n2 Cl37	1.96571	–	–	sp 99.99	0.03	99.97
–	-0.32654	–	–	–	–	–
n3 Cl37	1.96083	–	–	sp 1.00	0.00	100.0
–	-0.32349	–	–	–	–	–
n1 N38	1.89110	–	–	sp 8.50	10.53	89.47
–	-0.24811	–	–	–	–	–
n1 N47	1.74920	–	–	sp 1.00	0.00	100.0
–	-0.22627	–	–	–	–	–

^a ED/e is expressed in a.u.

benzene, and piperazine groups makes it the most reactive part in the molecule.

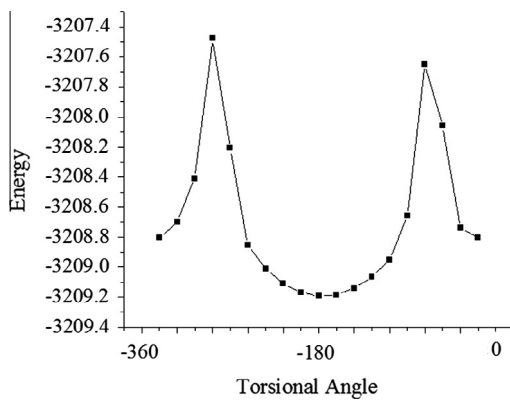
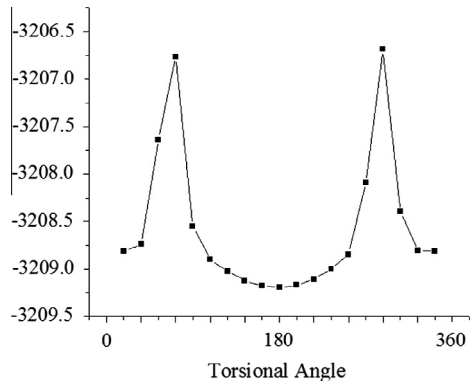
HOMO–LUMO band gap

HOMO and LUMO are the very important parameters for quantum chemistry. The conjugated molecules are characterized by a highest occupied molecular orbital–lowest unoccupied molecular orbital (HOMO–LUMO) separation, which is the result of a

significant degree of ICT from the end-capping electron-donor groups to the efficient electron-acceptor groups through π-conjugated path. The strong charge transfer interaction through π-conjugated bridge results in substantial ground state donor–acceptor mixing and the appearance of a charge transfer band in the electronic absorption spectrum. Therefore, an ED transfer occurs from the more aromatic part of the π-conjugated system in the electron donor side to its electron-withdrawing part. The atomic orbital components of the frontier molecular orbital are given in Figs. S4

Table 3Experimental and calculated ^1H NMR parameters (with respect to TMS).

Proton	σ_{TMS}	B3LYP/6-31G σ_{calc}	$\delta_{\text{calc}} \cdot (\sigma_{\text{TMS}} - \sigma_{\text{calc}})$	Exp. δ_{ppm}
H10	32.7711	29.1949	3.5762	3.65
H12		29.3181	3.4530	3.65
H20		29.0239	3.7472	3.65
H21		28.8704	3.9007	3.65
H22		29.0295	3.7416	3.65
H23		29.1431	3.6208	3.65
H24		29.1318	3.6393	3.65
H25		29.0616	3.7095	3.59
H26		29.1606	3.6105	3.59
H27		29.0454	3.7257	3.65
H29		30.7268	2.0443	2.16
H30		30.6984	2.0727	2.18
H32		30.0619	2.7092	2.45
H33		29.2889	3.4822	3.50
H41		29.2599	3.5112	3.54
H42		29.2081	3.5630	3.55
H43		29.0796	3.6915	3.72
H44		29.0874	3.6837	3.72
H48		28.8471	3.9240	3.74
H49		29.0241	3.747	3.73
H50		28.9501	3.8270	3.74
H51		28.8454	3.9257	3.74
H56		25.7521	7.019	7.01
H58		25.7518	7.0193	7.00
H60		25.3483	7.4228	7.33
H61		25.9348	6.8363	6.99
H62		25.3925	7.3786	7.29

**Fig. 4.** Profile of potential energy scan for the torsion angle C31–C28–C19–N15.**Fig. 5.** Profile of potential energy scan for the torsion angle N38–C31–C28–C19.

and S5 as Supporting material. The HOMO–LUMO energy gap value is found to be 3.182 eV, which is responsible for the bioactive property of the compound TDPPAD, as reported in the literature [92–94].

Conclusion

FT-IR and FT-Raman spectra of TDPPAD were recorded and analyzed. The vibrational wavenumbers were computing at various levels of theory. The data obtained from theoretical calculations are used to assign vibrational bands obtained experimentally. The geometrical parameters of the title compound are in agreement with that of similar derivatives. In addition, the calculated ^1H NMR is all in good agreement with the experimental data. The lowering of HOMO–LUMO band gap supports bioactive property of the molecule. MEP predicts the most reactive part in the molecule. The calculated first hyperpolarizability is comparable with the reported values of similar derivatives and is an attractive object for future studies of non-linear optics.

Acknowledgements

The authors are thankful to University of Antwerp for access to the university's CalcUA Supercomputer Cluster. RR thanks University Grants Commission, India, for a research fellowship.

Appendix A. Supplementary material

Supplementary data associated with this article can be found, in the online version, at <http://dx.doi.org/10.1016/j.saa.2014.01.045>.

References

- [1] L.H. Atherton, Bentley and Driver's Text Book of Pharmaceutical Chemistry, eighth ed., Oxford Medicinal Publication, 2004. pp. 372–377, 204–205.
- [2] A.H. Beckett, J.B. Stenlake, Practical Pharmaceutical Chemistry, fourth ed., CBS Publishers and Distributors, 2003.
- [3] R.S. Upadhyaya, N. Sinha, S. Jain, N. Kishore, R. Chandra, S.K. Arora, Bioorg. Med. Chem. 12 (2004) 2225–2238.
- [4] W.O. Foye, T.L. Lemke, D.A. Willard, Principles of Medicinal Chemistry, fourth ed., Williams and Wilkins, London, 1995.
- [5] L.L. Gan, Y.H. Lu, C.H. Zhou, Chin. J. Biochem. Pharm. 30 (2009) 127–131.
- [6] J.L. Cai, Y.H. Lu, L.L. Gan, C.H. Zhou, Chin. J. Antibiotics 34 (2009) 454–462.
- [7] L.L. Gan, J.L. Cai, C.H. Zhou, Chin. Pharm. J. 44 (2009) 1361–1368.
- [8] O.A. Phillips, E.E. Udo, S.M. Samuel, Eur. J. Med. Chem. 43 (2008) 1095–1104.
- [9] A. Foroumadi, S. Emami, S. Mansouri, A. Javidnia, N. Saeid-Adeli, F.H. Shirazi, A. Shafiee, Eur. J. Med. Chem. 42 (2007) 985–992.
- [10] B.B. Lohray, V.B. Lohray, B.K. Srivastava, S. Gupta, M. Solanki, P. Pandya, P. Kapadnis, Bioorg. Med. Chem. Lett. 16 (2006) 1557–1561.
- [11] A. Foroumadi, S. Ghodsi, S. Emami, S. Najjari, N. Samadi, M.A. Faramarzi, L. Beikmohammadi, F.H. Shirazi, A. Shafiee, Bioorg. Med. Chem. Lett. 16 (2006) 3499–3503.
- [12] W.J. Watkins, L. Chong, A. Cho, R. Hilgenkamp, M. Ludwikow, N. Garizi, N. Iqbal, J. Barnard, R. Singh, D. Madsen, K. Lolans, O. Lomovskaya, U. Oza, P. Kumaraswamy, A. Blecken, S. Bai, D.J. Loury, D.C. Griffith, M.N. Dudley, Bioorg. Med. Chem. Lett. 17 (2007) 2802–2806.
- [13] L.L. Rokosz, C.Y. Huang, J.C. Reader, T.M. Stauffer, D. Chelsky, N.H. Sigal, A.K. Ganguly, J. Baldwin, J. Bioorg. Med. Chem. Lett. 15 (2005) 5537–5543.
- [14] J.J. Chen, M. Lu, Y.K. Jing, J.H. Dong, Bioorg. Med. Chem. 14 (2006) 6539–6547.
- [15] P.J. Shami, J.E. Saavedra, C.L. Bonifant, J.X. Chu, V. Udupi, S. Malaviya, B.I. Carr, S. Kar, M.F. Wang, L. Jia, X.H. Ji, L.K. Keefer, J. Med. Chem. 49 (2006) 4356–4366.
- [16] A. Mayence, J.J.V. Eynde, L. LeCour Jr., L.A. Walker, B.L. Tekwani, T.L. Huang, Eur. J. Med. Chem. 39 (2004) 547–553.
- [17] W. Cunico, C.R.B. Gomes, M. Moreth, D.P. Manhanini, I.H. Figueiredo, I.C. Penido, M.G.M.O. Henriques, F.P. Varotti, A.U. Krettl, Eur. J. Med. Chem. 44 (2009) 1363–1368.
- [18] R.A. Smits, H.D. Lim, A. Hanzer, O.P. Zuiderveld, E. Guaita, M. Adami, G. Coruzzi, R. Leurs, I.P.J. Esch, J. Med. Chem. 51 (2008) 2457–2467.
- [19] J. Penjišević, V. Šukalović, D. Andrić, S. Kostić-Rajačić, V. Šoškić, G. Roglić, Arch. Pharm. Chem. Life Sci. 340 (2007) 456–465.
- [20] O.M. Becker, D.S. Dhanoa, Y. Marantz, D. Chen, S. Shacham, S. Cheruku, A. Heifetz, P. Mohanty, M. Fichman, A. Sharadendu, R. Nudelman, M. Kauffman, S. Noiman, J. Med. Chem. 49 (2006) 3116–3135.
- [21] D.C. Bean, D.W. Wareham, J. Antimicrob. Chemother. 63 (2009) 349–352.
- [22] A.Y. Coban, Z. Bayram, F.M. Sezgin, B. Durupinar, Bull. Microbiol. 43 (2009) 457–461.
- [23] P. Chaudhary, R. Kumar, A.K. Verma, D. Singh, V. Yadav, A.K. Chhillar, G.L. Sharmak, R. Chandra, Bioorg. Med. Chem. 14 (2006) 1819–1826.
- [24] V.M. Farzaliiev, M.T. Abbasova, A.A. Ashurova, G.B. Babaeva, N.P. Ladokhina, Y.M. Kerimova, Russ. J. Appl. Chem. 82 (2009) 928–930.
- [25] J. Stefańska, A. Bielenica, M. Struga, S. Tyski, J. Kossakowski, P.L. Colla, E. Tamburini, R. Loddo, Ann. Microbiol. 60 (2010) 151–155.

- [26] C.Y. Panicker, H.T. Varghese, K.M. Pillai, Y.S. Mary, K. Raju, T.K. Manojkumar, A. Bielenica, C. Van Alsenoy, *Spectrochim. Acta* 75 (2010) 1559–1565.
- [27] H.T. Varghese, C.Y. Panicker, K.M. Pillai, Y.S. Mary, K. Raju, T.K. Manojkumar, A. Bielenica, C. Van Alsenoy, *Spectrochim. Acta* 76 (2010) 513–522.
- [28] J. Kossakowski, A. Bielenica, B. Miroslaw, A.E. Koziol, I. Dybał, M. Struga, *Molecules* 13 (2008) 1570–1583.
- [29] R. Filosa, A. Peduto, P. de Capraris, C. Saturnino, M. Festa, A. Petrella, A. Pau, G.A. Pinna, P.L. Colla, B. Busonera, R. Loddio, *Eur. J. Med. Chem.* 42 (2007) 293–306.
- [30] C.A. Peri, *Gazz. Chim. Ital.* 85 (1955) 1118–1140.
- [31] J. Kossakowski, M. Pakosinska-Parrys, M. Struga, I. Dybał, A.E. Koziol, P. LaColla, L.E. Marongiu, C. Ibba, D. Collu, R. Loddio, *Molecules* 14 (2009) 5189–5202.
- [32] M.J. Frisch, G.W. Trucks, H.B. Schlegel, G.E. Scuseria, M.A. Robb, J.R. Cheeseman, G. Scalmani, V. Barone, B. Mennucci, G.A. Petersson, H. Nakatsuji, M. Caricato, X. Li, H.P. Hratchian, A.F. Izmaylov, J. Bloino, G. Zheng, J.L. Sonnenberg, M. Hada, M. Ehara, K. Toyota, R. Fukuda, J. Hasegawa, M. Ishida, T. Nakajima, Y. Honda, O. Kitao, H. Nakai, T. Vreven, J.A. Montgomery Jr., J.E. Peralta, F. Ogliaro, M. Bearpark, J.J. Heyd, E. Brothers, K.N. Kudin, V.N. Staroverov, T. Keith, R. Kobayashi, J. Normand, K. Ragahavachari, A. Rendell, J.C. Burant, S.S. Iyengar, J. Tomasi, M. Cossi, N. Rega, J.M. Millam, M. Klene, J.E. Knox, J.B. Cross, V. Bakken, C. Adamo, J. Jaramillo, R. Gomperts, R.E. Stratmann, O. Yazyev, A.J. Austin, R. Cammi, C. Pomelli, J.W. Ochterski, R.L. Martin, K. Morokuma, V.G. Zakrzewski, G.A. Voth, P. Salvador, J.J. Dannenberg, S. Dapprich, A.D. Daniels, O. Farkas, J.B. Foresman, J.V. Ortiz, J. Cioslowski, D.J. Fox, Gaussian 09, Revision B.01, Gaussian Inc., Wallingford CT, 2010.
- [33] J.B. Foresman, in: E. Frisch (Ed.), *Exploring Chemistry with Electronic Structure Methods: A Guide to Using Gaussian*, Gaussian Inc., Pittsburg, PA, 1996.
- [34] P.J. Hay, W.R. Wadt, *J. Chem. Phys.* 82 (1985) 270–283.
- [35] J.Y. Zhao, Y. Zhang, L.G. Zhu, *J. Mol. Struct. Theochem.* 671 (2004) 179–187.
- [36] R. Dennington, T. Keith, J. Millam, *GaussView*, Version 5, Semichem Inc., Shawnee Mission KS, 2009.
- [37] J.M.L. Martin, C.V. Alsenoy, GAR2PED, A Program to Obtain a Potential Energy Distribution from a Gaussian Archive Record, University of Antwerp, Belgium, 2007.
- [38] N.P.G. Roeges, *A Guide to the Complete Interpretation of Infrared Spectra of Organic Structures*, Wiley, New York, 1994.
- [39] G. Varsanyi, *Assignments of Vibrational Spectra of Seven Hundred Benzene Derivatives*, Wiley, New York, 1974.
- [40] N.B. Colthup, L.H. Daly, S.E. Wiberly, *Introduction to Infrared and Raman Spectroscopy*, Academic Press, New York, 1990.
- [41] A. Kuwae, K. Machida, *Spectrochim. Acta A* 34A (1978) 785–791.
- [42] S. Higuchi, H. Tsuyama, S. Tanaka, H. Kamada, *Spectrochim. Acta A* 30A (1974) 463–467.
- [43] J. Klimentova, P. Vojtisek, M. Sklenarova, *J. Mol. Struct.* 871 (2007) 33–41.
- [44] I.C.H. Castaneda, J.L. Jios, O.E. Piro, G.E. Tobon, C.O.D. Vedova, *J. Mol. Struct.* 842 (2007) 46–54.
- [45] R. Zhang, X. Li, X. Zhang, *Front. Chem. China* 6 (2011) 358–366.
- [46] G. Socrates, *Infrared Characteristic Group Frequencies*, John Wiley and Sons, New York, 1981.
- [47] I.N. Tarabara, Y.S. Bondarenko, A.A. Zhurakovskii, L.I. Kas'yan, *Russ. J. Org. Chem.* 43 (2007) 1297–1304.
- [48] K. Nakanishi, *Infrared Absorption Spectroscopy Practical*, Holden-Day, San Francisco, 1962.
- [49] S. Kundoo, A.N. Banerjee, P. Saha, K.K. Chattophayay, *Mater. Lett.* 57 (2003) 2193–2197.
- [50] M. Silverstein, G.C. Basseler, C. Morill, *Spectrometric Identification of Organic Compounds*, Wiley, New York, 1981.
- [51] L.I. Kas'yan, A.V. Serbin, A.O. Kas'yan, D.V. Karpenko, E.A. Golodaeva, *Russ. J. Org. Chem.* 44 (2008) 340–347.
- [52] L.H. Daly, S.E. Wiberly, *Introduction to Infrared and Raman Spectroscopy*, third ed., Academic Press, Boston, 1990.
- [53] Y.M. Atroshchenko, I.V. Shakhkeldyan, O.V. Leonova, A.N. Shumskii, N.A. Troitskii, I.E. Yakunina, A.N. Shchukin, Y.A. Efremov, *Russ. J. Org. Chem.* 41 (2005) 1212–1218.
- [54] C. Lee, W. Yang, R.G. Parr, *Phys. Rev.* 37B (1988) 785–789.
- [55] E.F. Mooney, *Spectrochim. Acta* 20 (1964) 1021–1032.
- [56] E.F. Mooney, *Spectrochim. Acta* 19 (1963) 877–887.
- [57] N. Sundaraganesan, C. Meganathan, B.D. Joshua, P. Mani, A. Jayaprakash, *Spectrochim. Acta* 71A (2008) 1134–1139.
- [58] P. Pazdera, H. Divisova, H. Havilsova, P. Borek, *Molecules* 5 (2000) 189–194.
- [59] P. Pazdera, H. Divisova, H. Havilsova, P. Borek, *Molecules* 566 (2000) 1166–1174.
- [60] H.T. Varghese, C.Y. Panicker, D. Philip, P. Pazdera, *Spectrochim. Acta* 67A (2007) 1055–1059.
- [61] H. Arslan, U. Florke, N. Kulcu, G. Binzet, *Spectrochim. Acta* 68A (2007) 1347–1355.
- [62] W.O. George, P.S. McIntyre, *Infrared Spectroscopy*, first ed., John Wiley and Sons, Chichester, 1987.
- [63] M.A. Palafox, V.K. Rastogi, L. Mittal, *Int. J. Quantum Chem.* 94 (2003) 189–204.
- [64] M. Kurt, *J. Raman Spectrosc.* 40 (1) (2009) 67–75.
- [65] K. Felfoldi, M. Sutyinszky, N. Nagy, I. Palinko, *Synth. Commun.* 30 (2000) 1543–1553.
- [66] A.A. El-Emam, A.S. Al-Tamimi, K.A. Al-Rashood, H.N. Misra, V. Narayan, O. Prasad, L. Sinha, *J. Mol. Struct.* 1022 (2012) 49–60.
- [67] H.L. Spell, *Anal. Chem.* 41 (1969) 902–905.
- [68] M.A.S. da Silva, S. Pinheiro, T. Francisco, F.O.N. da Silva, A.A. Batista, J. Ellena, I.M.M. Carvalho, J.R. de Sousa, F.A. Dias-Filho, E. Longhinotti, I.C.N. Diógenes, *J. Braz. Chem. Soc.* 21 (2010) 1754–1759.
- [69] N.R. Conley, R.J. Hung, C.G. Willson, *J. Org. Chem.* 70 (2005) 4553–4555.
- [70] T.M.V.D. Pinho e Melo, A.M.T.D.P. Cabral, A.M.R. Gonsalves, A.M. Beja, J.A. Paixao, M.R. Silva, L.A. daVeiga, *J. Org. Chem.* 64 (1999) 7229–7232.
- [71] D. Lee, T.M. Swager, *Chem. Mater.* 17 (2005) 4622–4629.
- [72] B. Bartkowska, F.M. Bohnen, C. Kruger, W.F. Maier, *Acta Crystallogr. C* 53 (1997) 521–522.
- [73] H.B. Burgi, J.D. Dunitz, *Structure Correlation*, vol. 2, VCH, Weinheim, 1994. pp. 741–784.
- [74] R. Manohar, M. Harikrishna, C.R. Ramanathan, M.S. Kumar, K. Gunasekaran, *Acta Crystallogr. E* 67 (2011) 1708.
- [75] L.I. Kas'yan, V.A. Palchikov, A.V. Turov, S.A. Pridma, A.V. Tokar, *Russ. J. Org. Chem.* 45 (2009) 1007–1017.
- [76] L.I. Kas'yan, S.V. Sereda, K.A. Poteknina, A.O. Kas'yan, *Heteroatom Chem.* 8 (1997) 177–184.
- [77] Z. Karczmarzyk, W. Malinka, *X-ray Struct. Anal.* 23 (2007) 151–152.
- [78] Y.R. Shen, *The Principles of Nonlinear Optics*, Wiley, New York, 1984.
- [79] P.V. Kolinsky, *Opt. Eng.* 31 (1992) 11676–11684.
- [80] D.F. Eaton, *Science* 25 (1991) 281–287.
- [81] D.A. Kleinman, *Phys. Rev.* 126 (1962) 1977–1979.
- [82] L.N. Kuleshova, M.Y. Antipin, V.N. Khrustalev, D.V. Gusev, E.S. Bobrikova, *Kristallografiya* 48 (2003) 594–601.
- [83] M. Adant, L. Dupuis, L. Bredas, *Int. J. Quantum Chem.* 56 (2004) 497–507.
- [84] E.D. Glendening, A.E. Reed, J.E. Carpenter, F. Weinhold, *NBO Version 3.1*, Gaussian Inc., Pittsburgh, PA, 2003.
- [85] J. Choo, S. Kim, H. Joo, Y. Kwon, *J. Mol. Struct. (Theochem.)* 587 (1) (2002) 1–8.
- [86] R.S. Mulliken, *J. Chem. Phys.* 23 (1955) 1833–1840.
- [87] K. Wolinski, J.F. Hinton, P. Pulay, *J. Am. Chem. Soc.* 112 (1990) 8251–8260.
- [88] E. Scrocco, J. Tomasi, *Adv. Quantum Chem.* 103 (1978) 115–121.
- [89] F.J. Luque, J.M. Lopez, M. Orozco, *Theor. Chem. Acc.* 103 (2000) 343–345.
- [90] P. Politzer, J.S. Murray, in: D.L. Beveridge, R. Lavery (Eds.), *Theoretical Biochemistry and Molecular Biophysics: A Comprehensive Survey*, Protein, vol. 2, Adenine Press, Schenectady, New York, 1991.
- [91] E. Scrocco, J. Tomasi, *Curr. Chem.* 7 (1973) 95–170.
- [92] Y. Li, Y. Liu, H. Wang, X. Xiong, P. Wei, F. Li, *Molecules* 18 (2013) 877–893.
- [93] H. Marouani, N. Raouafi, S. ToumiAkriche, S.S. Al-Deyab, M. Rzaigu, E.-J. Chem. 9 (2012) 772–779.
- [94] B.A. Saeed, R.S. Elias, S.M.H. Ismael, K.A. Hussain, *Am. J. Appl. Sci.* 8 (2011) 773–776.